University of the Witwatersrand

Quasinormal modes for spin-3/2 particles in N-dimensional Schwarzschild black hole space times

Author:
Mr. Gerhard Harmsen

Supervisor:
Prof. Alan S. Cornell

A dissertation submitted in fulfilment of the requirements for the degree of Masters

in the

Mandelstam Institute for Theoretical Physics,
School of Physics, University of the Witwatersrand

June 2016

Abstract

This dissertation will focus on spin-3/2 perturbations on N-dimensional Schwarzschild black holes, with the aim of calculating the numerical values for the quasi-normal modes (QNMs) and absorption probabilities associated with these perturbations. We begin by determining the spinor-vector eigenmodes of our particles on an (N-2)-dimensional spherical background. This allows us to separate out the angular part and radial part on our N-dimensional Schwarzschild metric. We then determine the equations of motion and effective potential of our particles near the N-dimensional black hole. Using techniques such as the Wentzel-Kramers-Brillouin and Improved Asymptotic Iterative Method we determine our QNMs and absorption probabilities. We see that higher dimensional black holes emit QNMs with larger real and imaginary values, this would imply they emit higher energy particles but that these particles are highly dampened and therefore would be difficult to detect. The results of the QNMs make sense if we also consider the effective potential surrounding our black holes with the potential function increasing with increasing number of dimensions.

Declaration of Authorship

I, Mr. Gerhard Harmsen, declare that this dissertation entitled, 'Quasinormal modes for spin-3/2 particles in N-dimensional Schwarzschild black hole space times' and the work presented in it are my own. I confirm that:

- This work was done wholly or mainly while in candidature for a research degree at this University.
- Where any part of this thesis has previously been submitted for a degree or any other qualification at this University or any other institution, this has been clearly stated.
- Where I have consulted the published work of others, this is always clearly attributed.
- Where I have quoted from the work of others, the source is always given. With the exception of such quotations, this thesis is entirely my own work.
- I have acknowledged all main sources of help.
- Where the thesis is based on work done by myself jointly with others, I have made clear exactly what was done by others and what I have contributed myself.

Signed: _____

Date: _____

Preface

The work in this dissertation is presented in the following published papers:

Articles

- Results which looked at the 4-dimensional space time are part of our work entitled "Gravitino fields in Schwarzschild black hole spacetimes" published in the Chinese Journal of Physics issue No.6, Vol. 53 Ref.[31].

Pre-print articles

- Large parts of chapters 2, 3, 4 and 5 are from a paper on spin-3/2 particles in D-dimensional Schwarzschild space times which has been uploaded to the arXiv (WITS-MITP-022), entitled "Spin-3/2 fields in D-dimensional Schwarzschild black hole space-times" Ref.[29]. We hope to have this paper published in the near future.

Proceedings

- A discussion of quasi-normal modes from black holes and methods of calculating these quasi-normal modes is presented in a proceedings to be published for the 2015 HEPP workshop entitled "Quasi-normal Modes for Spin-3/2 Fields" in the Journal of Physics: Conference Series Vol. 645 Ref.[21].

- A discussion of absorption probabilities for N-dimensional black holes is given in a soon to be published proceedings for the 2016 HEPP workshop entitled "Absorption probabilities associated with spin-3/2 particles near N-dimensional Schwarzschild black holes" pre-print arXiv:1602.07434 Ref.[43].

Acknowledgements

I would like to thank Wade Naylor for his useful discussions during the production of this work. This work was supported in part by the National Research Foundation of South Africa (Grant No: 91549). I would like to thank Chung-Hung Chen and Hing-Tong Cho for their hospitality during my visit to Tamkang University, where part of this work was completed. I would also like to thank my supervisor Prof. Alan Cornell for all his help during my masters studies and for allowing me to visit Taiwan during my studies. I would also like to thank Mr. Warren Carlson, currently a PhD student at the University of the Witwatersrand, for his help in explaining some of the concepts required to complete my masters studies. I would also like to thank my parents for all their support during my studies.

"I don't want to believe. I want to know"

Carl Sagan

Contents

List of Tables

List of Figures

Chapter 1

Introduction

In June 2015 the Large Hadron Collider was able to produce collisions with an energy of 13 TeV, where collisions at these energy levels may allow for the formation of higher dimensional black holes [1, 2]. One way of detecting the formation, and decay, of these black holes would be to study the quasi-normal modes (QNMs) of these black holes. The QNMs emitted from black holes can be used to determine the parameters of the black holes from which they were emitted. Furthermore a study of their absorption probabilities would provide insight into the particle emission of these black holes. However, these black holes could only form if the ideas from supersymmetric theories are correct. Recall that supersymmetric theories use spinors, and their relation to particle spin, to show that fermionic fields can be related to bosonic fields and vice versa. In supergravity theories we make the assumption that the graviton mediates gravitational forces and that its supersymmetric partner is the gravitino, a spin-3/2 particle. Most of the research related to the gravitino is focused on the particle itself and not no how it interacts with the space time. In our research we focus on how spin-3/2 particles, such as the gravitino, are affected by N-dimensional Schwarzschild black holes by studying their QNMs and absorption probabilities. In the next few sections we give a more elaborate explanation of how spinors are related to particles and how their applications in supersymmetry result in a fermionic and bosonic symmetry. Using this we motivate the existence of the gravitino and how we calculate its associated QNMs and absorption probabilities.

1.1 Spinors

Spinors are complex vector-like objects which can be attributed to some metric space. Under infinitesimal rotations of this metric space our spinors would behave just like

ordinary vectors, however for sequential rotations of our space the spinors behave very differently. They are in fact sensitive to the order in which the rotations take place as well as the result of our infinitesimal rotations, which is not true of the vectors or tensors we could associate to our metric space [3]. In this paper we construct our spinors as follows

$$\psi = \begin{pmatrix} \psi_1 \\ \psi_2 \\ \vdots \\ \psi_D \end{pmatrix} , \tag{1.1}$$

where $D = N$ when N is even and $D = N - 1$ when N is odd, and the ψ_i's represent our spinor components [4]. In the 1920's Dirac discovered that spinors were necessary to describe spin-1/2 subatomic particles. He discovered this while trying to find a relativistic form of the Schrödinger equation that was first order in time, the equation that he derived is now subsequently named the Dirac equation [5]. The Dirac equation is given as follows

$$i\hbar\gamma^\mu\partial_\mu\Psi - mc\Psi = 0 \, , \tag{1.2}$$

where γ^μ is the gamma matrix which obeys the Clifford algebra and is defined by the following anticommutation relation

$$\{\gamma^\mu, \gamma^\nu\} = 2g^{\mu\nu} \, , \tag{1.3}$$

with $g^{\mu\nu}$ representing our metric. This means our wave function must be some vector-like object with dimensions equal to the gamma matrix. In 4 dimensions it is given as

$$\Psi = \begin{pmatrix} \Psi_1 \\ \Psi_2 \\ \Psi_3 \\ \Psi_4 \end{pmatrix} , \tag{1.4}$$

where using a Weyl representation allows us to rewrite it as

$$\Psi = \begin{pmatrix} \psi \\ \chi \end{pmatrix} . \tag{1.5}$$

ψ and χ are eigenstates of γ^5 in that

$$\gamma^5 \begin{pmatrix} \psi \\ 0 \end{pmatrix} = \begin{pmatrix} \psi \\ 0 \end{pmatrix} , \quad \text{and} \quad \gamma^5 \begin{pmatrix} 0 \\ \chi \end{pmatrix} = - \begin{pmatrix} 0 \\ \chi \end{pmatrix} . \tag{1.6}$$

Since the eigenstates of γ^5 matrices represent chirality we can think of ψ as representing right handed particles and χ representing left handed particles [6].

1.2 Supersymmetry

By the 1960's the Standard Model (SM) was a well established theory, and had been successful at not only explaining particle behaviour but also at predicting new particles and their behaviour [5]. We therefore knew that there existed the Poincaré symmetry, given by the Lorentz generators J_{ab}, SO(1,3), and the generators of the 3+1 dimensional translation symmetries. We also knew that there existed internal symmetries such as the U(1) symmetry of electromagnetism, SU(3) of quantum chromodynamics and the SU(2) of weak isospin. The next step was to determine if these symmetries could be combined in some way. It turns out that it is not possible to combine these symmetries if we assume that the final algebra must be a Lie algebra. We can, however, obtain better results if we instead use a graded Lie algebra to construct the symmetric relations [7]. The generators of this group are denoted as Q and are spinor quantities which in a Weyl representation are written as [6]

$$Q = \begin{pmatrix} Q_1 \\ Q_2 \end{pmatrix} , \tag{1.7}$$

where the anticommutation relations of our components are

$$\{Q_a, Q_b\} = 0 \, , \{Q_a^\dagger, Q_b^\dagger\} = 0 \text{ and } \{Q_a, Q_b^\dagger\} = (\sigma^\mu)_{ab} \, P_\mu \, , \tag{1.8}$$

where the subscripts for σ^μ denote the particular elements of that matrix, and P_μ represents the momentum operator. Commutations of these generators with the rotation generators, J_μ, and the momentum operator, P_μ, are as follows,

$$[J_3, Q_1] = -\frac{1}{2} Q_1 \quad \text{and} \quad [J_3, Q_2] = \frac{1}{2} \, , \tag{1.9}$$

$$[Q_a, P_\mu] = \left[Q_a^\dagger, P_\mu^\dagger \right] = 0 \, . \tag{1.10}$$

Since our Q's are quantum operators this tells us that Q_1 would lower the spin of a particle by 1/2 and Q_2 would raise the value by 1/2 and would leave the mass of the particle

unchanged [6]. We therefore have a coupling between bosonic fields and fermionic fields which implies that for every particle there exists a supersymmetric partner which has the same mass but differs in spin by exactly 1/2.

1.2.1 Supergravity

Supergravity theories are theories that combine the properties of supersymmetry with those of general relativity. In these theories the gravitino would be the supersymmetric partner of the hypothetical graviton, which is expected to be the quantum of the gravitational field. The graviton is expected to be a massless spin-2 particle which would mediate the gravitational force [8]. As such its supersymmetric partner, the gravintino, would have to be a spin-3/2 fermion and would behave like a Rarita-Schwinger field [7].

1.2.2 Gravitino

In supergravity theories the gravitinos mass is related to the scale at which supersymmetry breaks. In order for supersymmetry to solve the hierarchy problem in the SM this would have to be no greater than 1 TeV [9, 10]. This restriction on the mass of the gravitino, however, results in problems for the standard model of cosmology. We can resolve some of these problems by assuming that the gravitino is the lightest supersymmetric particle and slightly violates R-parity when it decays [11].

1.3 Higher dimensional black holes

Although supergravity theories do not require extra dimensions to exist, many of them have been extended to dimensions larger than 4. If these higher dimensional supergravity theories are correct, then it should be possible for higher dimensional black holes to exist, where the existence of 4-dimensional black holes is predicted by general relativity. These higher dimensional black holes should theoretically form at the LHC when it produces collisions with energies on the order of the TeV scale [12–14]. As yet no black holes have been detected at either the LHC, or any other particle accelerator, even though they are producing collisions with energies in the TeV scale. It is suspected that this is due to the incorrect interpretation of quantum gravity being used to predict the theoretical energies required to create these black holes. In Ref.[15] the gravity rainbow theory is used to explain why higher dimensional black holes have thus far not been detected and what the true energies to form these higher dimensional black holes might be. If these higher dimensional black holes are ever created in our particle colliders we would expect

them to emit a very unique spectrum of energy, using a field theoretic approach this would imply particle emission.

1.4 Absorption probabilities of black holes

Consider a system with only one particle, of energy ω, and a Schwarzschild black hole. If the only forces present are gravitational forces then classically we could describe this system using only the Schwarzshild metric. Furthermore, using the metric and the energy of the particle we could determine the probability of the particle being absorbed by the black hole. However, this probability is different when using a field-theoretic approach to study the system [16]. Unruh showed this difference in 1976, where he determined that an accelerating observer would observe black body radiation [17], this emitted radiation could be thought of as particle emissions. In this way the Unruh effect could be considered to be another way of showing the existence of Hawking radiation. In most field theories the emitted particles exhibit well defined resonances called QNMs and are uniquely determined by the black hole that emitted the particle.

1.5 Quasi normal modes

The study of QNMs related to black holes was started in the 1950's by Regge and Wheeler [18]. In their paper they studied the stability of Schwarzschild black holes after small perturbations were applied to them. They looked at the oscillations on the surface of the black hole as a way of measuring the stability of the perturbed black holes. These oscillations on the surface of the black hole have both a real (stable) and a non-real (unstable) frequency associated to them, these complex frequencies represent QNMs. While studying the scattering of gravitational waves off Schwarzschild black holes Vishveshwara [19] pointed out that QNMs were possibly being emitted from black holes into the space time surrounding the black hole. In this case the real part of the QNM represents the frequency and the imaginary part its damping term. A more intuitive example of what a QNM is can be presented by considering the tapping of a knife on a wine glass. If we tap the wine glass we are in fact perturbing the glass. This perturbation causes the glass to resonate at specific frequencies. The allowed frequencies are determined by the composition of the glass, and even the contents within the glass. If the glass continued to resonate forever then we would be generating a normal mode. Since the glass does stop resonating we say it is a QNM. So when studying QNMs we are studying standing waves with some damping term attached. If we consider our wine glass example we should note that wine glasses with different amounts of water in them

ring at different frequencies, so we could, in theory, determine the amount of water in a glass by the sound it makes when we tap the glass. A similar idea can be used for the emitted QNMs of a black hole. Except with the black holes it is reliant on the mass of the black hole which is emitting the particles. Below we present a more mathematical description of QNMs.

1.5.1 A Mathematical description of QNMs

In order to develop a more mathematical understanding of QNMs we can look at the mathematical formula for standing waves since, as stated above, QNMs are merely damped standing waves. So we can represent these QNMs as follows [19]

$$\frac{d^2}{dx^2}\Psi - \frac{d^2}{dt^2}\Psi - V\Psi = 0\,. \tag{1.11}$$

With Ψ describing some wavelike function where x and t denote space and time coordinates respectively, V is some x-dependent potential. We can solve the equation as we would a standing wave problem and so we can assume the following time dependency [20]:

$$\Psi(x,t) = e^{-i\omega t}\phi(x)\,. \tag{1.12}$$

Plugging this into our equation for a QNM we get

$$\frac{d^2\phi(x)}{dx^2} - \Big(\omega^2 + V(x)\Big)\phi(x) = 0\,. \tag{1.13}$$

This is the general form for the QNMs we will be studying in this paper. In order to solve this equation we require specific boundary terms, similar to those required for solving the standing wave equation. The boundary conditions that we will impose are:

$$\begin{aligned} V &\to 0 \quad ; \quad x \to \infty\,, \\ V &\to 0 \quad ; \quad x \to -\infty\,. \end{aligned} \tag{1.14}$$

This means that particles fall into the black hole at the horizon and those which move to infinity are no longer influenced by the black hole.

Once we have an equation of the form Eq.(1.13) we can use either numerical or semi-analytical techniques to determine the numerical solutions for our QNMs. In this dissertation we have chosen to use the Wentzel-Kramers-Brillouin (WKB) method and improved asymptotic iterative method (AIM). We describe how these two methods are implemented in the next few sections.

1.5.2 WKB Approximation

The WKB method is a well known approximation and is usually used in quantum mechanics to determine solutions to the Schrödinger equation in systems with non-constant potentials. Note that the WKB method can be used to determine the approximate solution to any second order differential equations of the Schrödinger form. In Ref.[[21]] we have given an example of how we use the WKB method to solve second order differential equations, we present this example below. We can use the WKB approximation to solve problems of the following form [22]

$$\epsilon^2 \frac{d^2y}{dx^2} = Q(x)y \,, \tag{1.15}$$

where $\epsilon \ll 1$. We can solve this equation by assuming the following solution

$$y(x,\epsilon) = A(x,\epsilon)e^{iu(x)/\epsilon} \,. \tag{1.16}$$

Taking the first and second derivatives of this function we see that

$$\begin{aligned}
y(x,\epsilon) &= A(x,\epsilon)e^{iu(x)/\epsilon} \,, \\
y'(x,\epsilon) &= A'(x,\epsilon)e^{iu(x)/\epsilon} + A(x,\epsilon)\left(\frac{iu'(x)}{\epsilon}\right)e^{iu(x)/\epsilon} \,, \\
y''(x,\epsilon) &= A''(x,\epsilon)e^{iu(x)/\epsilon} + A'(x,\epsilon)\left(\frac{iu'(x)}{\epsilon}\right)e^{iu(x)/\epsilon} + A'(x,\epsilon)\left(\frac{iu'(x)}{\epsilon}\right)e^{iu(x)/\epsilon} \\
&\quad - A(x,\epsilon)\left(\frac{u'(x)}{\epsilon}\right)^2 e^{iu(x)/\epsilon} \\
&= \left(A'' + 2A'\frac{iu'(x)}{\epsilon} + A(\frac{iu''(x)}{\epsilon} - \left(\frac{u'(x)}{\epsilon}\right)^2\right)e^{iu(x)/\epsilon} \,.
\end{aligned} \tag{1.17}$$

Plugging Eq.(1.17) into Eq.(1.15) we get

$$\epsilon^2\left(A'' + 2A'\frac{iu'(x)}{\epsilon} + A(\frac{iu''(x)}{\epsilon} - \left(\frac{u'(x)}{\epsilon}\right)^2\right) - Q(x)A(x,\epsilon) = 0 \,. \tag{1.18}$$

We now perform a series expansion on A as follows

$$\begin{aligned}
A(x,\epsilon) &= A_0(x) + \epsilon A_1(x) + \epsilon^2 A_2(x) + ... \\
A'(x,\epsilon) &= A_0'(x) + \epsilon A_1'(x) + \epsilon^2 A_2'(x) + ... \\
A''(x,\epsilon) &= A_0''(x) + \epsilon A_1''(x) + \epsilon^2 A_2''(x) + ...
\end{aligned} \tag{1.19}$$

so that Eq.(1.18) becomes

$$\epsilon^2\left(\left(A_0''(x)+\epsilon A_1''(x)+\epsilon^2 A_2''(x)+...\right)+2\left(A_0'(x)+\epsilon A_1'(x)+\epsilon^2 A_2'(x)+...\right)\frac{iu'(x)}{\epsilon}\right)+ \\ \epsilon^2\Big(\left(A_0(x)+\epsilon A_1(x)+\epsilon^2 A_2(x)+...\right)(\frac{iu''(x)}{\epsilon}-\left(\frac{u'(x)}{\epsilon}\right)^2 \\ -Q(x)\left(A_0(x)+\epsilon A_1(x)+\epsilon^2 A_2(x)+...\right)\Big)=0\,. \tag{1.20}$$

We then group the terms in powers of ϵ to get our approximation. So for instance we can collect all terms of ϵ^0 to get a solution to $u(x)$

$$\begin{aligned} A_0(x)u'(x)^2+A_0Q(x)&=0\,,\\ u'(x)&=\pm\sqrt{Q(x)}\,,\\ u(x)&=\pm\int_{x_0}^{x}\sqrt{Q(k)}dk\,. \end{aligned} \tag{1.21}$$

We then take orders of ϵ to get our first order approximation of A

$$\begin{aligned} -u'(x)^2A_1+iA_0u''(x)+2iA_0'u'(x)+Q(x)A_0&=0\,,\\ A_0u''(x)+2A_0'u'(x)&=0\,,\\ \frac{A_0}{2\sqrt{Q(x)}}+\frac{A_0'}{\sqrt{Q(x)}}&=0\,, \end{aligned} \tag{1.22}$$

$$\int\frac{1}{A_0}dA_0=\int\frac{1}{2Q(x)}dx\,. \tag{1.23}$$

We can use the WKB method in order to study black hole perturbations since these equations reduce to the form of a wave equation, similar to the example above [20]. This equation, with the known potential, is then solved using both the 3rd order in Ref.[23] and 6th order in Ref.[24] WKB approximations.

1.5.3 Improved AIM

We begin by describing the AIM as shown in Ref.[25] and then give motivation for updating this method as well as showing how the improved AIM was developed. The AIM allows us to solve equations of the form

$$y''=\lambda_0(x)y'+s_0(x)y\,, \tag{1.24}$$

where λ_0 and s_0 are in $C_\infty(a,b)$ [25]. Iteratively taking n derivatives of Eq.(1.24) we have an equation of the form

$$y^{(n+2)} = \lambda_n y' + s_n y \,, \tag{1.25}$$

where $\lambda_n = \lambda'_{n-1} + s_{n-1} + \lambda_0\lambda_{n-1}$ and $s_n = s'_{n-1} + s_0\lambda_{n-1}$. The taking the ratio of our $n+1$ derivative and $n+2$ derivative we have,

$$\frac{y^{(n+2)}}{y^{(n+1)}} = \frac{d}{dx}\ln(y^{(n+1)}) = \frac{\lambda_n(y' + \frac{s_n}{\lambda_n}y)}{\lambda_{n-1}(y' + \frac{s_{n-1}}{\lambda_{n-1}}y)} \,. \tag{1.26}$$

We can simplify this equation by defining [25]

$$\alpha = \frac{s_n}{\lambda_n} = \frac{s_{n-1}}{\lambda_{n-1}} \,, \tag{1.27}$$

which allows us to rewrite Eq.(1.26) as

$$\frac{d}{dx}\ln(y^{(n+1)}) = \frac{\lambda_n}{\lambda_{n-1}} \,. \tag{1.28}$$

Solving the above equation and plugging the solution into Eq.(1.24) we find that our solution for $y(x)$ is given as

$$y(x) = \exp\left(-\int^x \alpha dt\right)\left[C_2 + C_1\int^x \exp\left(\int^t (\lambda_0(\tau) + 2\alpha(\tau))\, d\tau\right)\right] \,, \tag{1.29}$$

where C_1 and C_2 are our integration constants. Clearly the iterative method for obtaining λ_n and s_n in order to find our α will be time consuming if n is very large. Since our QNMs are very sensitive to initial conditions we require α to a high degree of precision and therefore require a large n. For this reason the AIM was improved, by using a Taylor expansion to find λ_n and s_n. They are determined as follows [26]

$$\begin{aligned} \lambda_n(\xi) &= \sum_{i=0}^{\infty} c_n^i (x-\xi)^i \,, \\ s_n(\xi) &= \sum_{n}^{\infty} d_n^i (x-\xi)^i \,, \end{aligned} \tag{1.30}$$

where ξ is value around which the AIM is performed and c_n^i and d_n^i are our Taylor coefficients. Plugging these into the previous expressions for λ_n and s_n we have the

following recursion relation

$$\begin{aligned} c_n^i &= (i+1)c_{n-1}^{i+1} + d_{n-1}^i + \sum_{k=0}^{i} c_0^k c_{n-1}^{i-k} \,, \\ d_n^i &(i+1)d_{n-1}^{i+1} + \sum_{k=0}^{i} d_0^k c_{n-1}^{i-k} \,. \end{aligned} \tag{1.31}$$

We calculate the values of our QNMs by solving $d_n^0 c_{n-1}^0 - d_{n-1}^0 c_n^0 = 0$, where n represents the number of iteration we wish to perform.

1.6 Outline of dissertation

This dissertation will be set out as follows: In the next chapter we determine the eigenfunctions and eigenvalues associated with spinors and vector-spinors on an N-dimensional sphere. We then use the eigenvalues on a sphere to determine the effective potential of spin-3/2 particles in N-dimensional space times, this is done in chapter 3. In chapter 4 we describe methods for determining QNMs and present the results of our QNM calculations. In chapter 5 we look at the absorption probabilities for our spin-3/2 particles near N-dimensional Schwarzschild black holes. A discussion and conclusion is presented in chapter 6. In this dissertation we will set $G = c = 1$.

Chapter 2

Spin-3/2 eigenmodes on the N-sphere

We begin our study of spin-3/2 fields in spherically symmetric space times by determining their eigenvalues on a sphere. We will determine the eigenvalues for both the spinors and the spinor-vectors used to represent our spin-3/2 particles on N-dimesnional spheres (S^N). The eigenfunctions, and eigenvalues, of spinors on S^N have been determined by Camporesi and Higuchi in Ref. [27]. We present a review of this paper below and use the results from this paper to determine the eigenfunctions for our spinor-vectors. We begin with the mathematical background for working with spinors and spinor-vectors on S^N and determine the eigenvalues of spinors and spinor-vectors in Sec.2.2 and Sec.2.3 respectively.

2.1 Review of the S^N

The metric for S^N is given as

$$d\Omega_N = \sin^2\theta_N d\widetilde{\Omega}_{N-1} + d\theta_N \,, \tag{2.1}$$

where $d\widetilde{\Omega}_{N-1}$ is the metric of the $N-1$ sphere, all tilde terms will now represent terms from the $N-1$ sphere. Our non-zero Christoffel symbols are

$$\Gamma^{\theta_N}_{\theta_i\theta_j} = -\sin\theta_N\cos\theta_N\widetilde{g}_{\theta_i\theta_j} \;;\; \Gamma^{\theta_j}_{\theta_i\theta_N} = \cot\theta_N\widetilde{g}^{\theta_j}_{\theta_i} \;;\; \Gamma^{\theta_k}_{\theta_i\theta_j} = \widetilde{\Gamma}^{\theta_k}_{\theta_i\theta_j} \,. \tag{2.2}$$

Our covariant derivative is given as

$$\nabla_\mu\psi = \partial_\mu\psi + \omega_\mu\psi \,, \tag{2.3}$$

where ω_μ is the spin connection. The spin connection is defined as follows

$$\omega_\mu = \frac{1}{2}\omega_{\mu ab}\Sigma^{ab}, \tag{2.4}$$

where $\Sigma^{ab} = \frac{1}{4}\left[\gamma^a, \gamma^b\right]$ and $\omega_{\mu ab}$ is calculated as

$$\omega_{\mu ab} = e_a^\alpha \left(\partial_\mu e_{\alpha b} - \Gamma^\rho_{\mu\alpha} e_{\rho b}\right), \tag{2.5}$$

where e_a^α is our n-bein [27]. Elements of the n-bein allow us to translate components of a curved space time to components in an orthonormal basis. In the extremely curved space times near black holes it is not always possible to find an orthonormal basis as such the n-bein formalism can be very useful, since they allow us to easily convert to and from an orthonormal basis where our calculations are much simpler. The n-bein translates components of our curved space time to an orthonormal basis as follows [28]

$$g_{\mu\nu} = e^a_\mu e^b_\nu \delta_{ab}\,, \quad e^a_\mu e^\mu_b = \delta_{ab}\,, \quad e^a_\nu e^b_\mu = \delta_{\nu\mu}\,, \tag{2.6}$$

where Greek letters, μ, ν, ..., represent our world indices and Latin letters, a, b, $c, ...$ represent our Lorenze indices. In the case of S^N our n-beins are

$$e^{\theta_N}_N = 1\,, \quad e^{\theta_i}_i = \frac{1}{\sin(\theta)}\widetilde{e}^{\theta_i}_i\,. \tag{2.7}$$

Dirac gamma matrices on S^N and Dirac gamma matrices on our orthonormal basis are related as follows

$$\gamma^{\theta_i} = e^{\theta_i}_i \gamma^i = \frac{1}{\sin\theta_N}\widetilde{e}^{\theta_i}_i \gamma^i\,, \quad \gamma^{\theta_N} = e^{\theta_N}_N \gamma^N = \gamma^N\,, \tag{2.8}$$

where the orthogonal gamma matrices must obey the Clifford Algebra. Our gamma matrices differ for the N even spheres and N odd spheres and we therefore determine our spin connections and eigenvalues on a case by case basis in the following sections.

2.2 Eigenmodes of spinors on S^N

We begin by determining the eigenvalues of our spinors when N is even and then move on to the case where N is odd.

2.2.1 N even

In this case our gamma matrices are given as,

$$\gamma^N = \begin{pmatrix} 0 & \mathbb{1} \\ \mathbb{1} & 0 \end{pmatrix} \quad \text{and} \quad \gamma^i = \begin{pmatrix} 0 & i\widetilde{\gamma}^i \\ -i\widetilde{\gamma}^i & 0 \end{pmatrix} , \tag{2.9}$$

where $\mathbb{1}$ is the $2^{\frac{N-2}{2}}$ identity matrix. Our spin connection is then given as

$$\omega_{\theta_i} = \begin{pmatrix} \widetilde{\omega}_{\theta_i} + \frac{i}{2}\cos\theta_N \widetilde{\gamma}_{\theta_i} & 0 \\ 0 & \widetilde{\omega}_{\theta_i} - \frac{i}{2}\cos\theta_N \widetilde{\gamma}_{\theta_i} \end{pmatrix} . \tag{2.10}$$

Using the Dirac derivative given in Eq.(2.3) our spinor equation is

$$\begin{aligned} \gamma^\mu \nabla_\mu \psi_\lambda &= \gamma^\mu \left(\partial_\mu \psi_\lambda - \omega_\mu \psi_\lambda\right) \\ &= \left[\left(\partial_{\theta_N} + \frac{N-1}{2}\cot\theta_N\right)\gamma^N + \frac{i}{\sin\theta_N}\begin{pmatrix} 0 & 1 \\ -1 & 0 \end{pmatrix}\widetilde{\gamma}^{\theta_i}\widetilde{\nabla}_{\theta_i}\right]\psi_\lambda = i\lambda\psi_\lambda . \end{aligned} \tag{2.11}$$

We can choose to express ψ_λ as

$$\psi_\lambda = \begin{pmatrix} \psi_\lambda^{(1)} \\ \psi_\lambda^{(2)} \end{pmatrix} = \begin{pmatrix} A_\lambda(\theta_N)\widetilde{\psi}_\lambda \\ -iB_\lambda(\theta_N)\widetilde{\psi}_\lambda \end{pmatrix} , \tag{2.12}$$

where $\widetilde{\psi}_\lambda$ is the eigenspinor for the surface of S^{N-1} satisfying

$$\widetilde{\gamma}^\mu \widetilde{\nabla}_\mu \widetilde{\psi}_\lambda = i\widetilde{\lambda}\widetilde{\psi}_\lambda ; \quad \widetilde{\lambda} = \pm\left(l + \frac{N-1}{2}\right) . \tag{2.13}$$

Plugging Eq.(2.12) into Eq.(2.11) we find that

$$\begin{aligned} \left(\partial_{\theta_N} + \frac{N-1}{2}\cot\theta_N + \frac{\widetilde{\lambda}}{\sin\theta_N}\right) A_\lambda &= \lambda B_\lambda , \\ \left(\partial_{\theta_N} + \frac{N-1}{2}\cot\theta_N - \frac{\widetilde{\lambda}}{\sin\theta_N}\right) B_\lambda &= -\lambda A_\lambda . \end{aligned} \tag{2.14}$$

We can solve this by expressing B_λ in terms of a Jacobi polynomial and relate it to A_λ as follows

$$\begin{aligned} B_\lambda(\theta_N) &= \left(\cos\frac{1}{2}\theta_N\right)^l \left(\sin\frac{1}{2}\theta_N\right)^{l+1} P_{n-l}^{((N/2)+l,(N/2)+l-1)}(\cos\theta_N) \\ &= (-1)^{n-l} A_\lambda(\pi - \theta_N) . \end{aligned} \tag{2.15}$$

In order for our Jacobi polynomial to converge we require that $(n-l) \geq 0$, the eigenvalue can then be written as

$$i\lambda = \pm i\left(n + \frac{N}{2}\right),\ n = 0, 1, 2, ..., \tag{2.16}$$

which is consistent with Eq.(2.13).

2.2.2 N odd

In the case where N is odd our gamma matrices are given as

$$\gamma^N = \begin{pmatrix} \mathbb{1} & 0 \\ 0 & \mathbb{1} \end{pmatrix}\ ;\quad \gamma^i = \widetilde{\gamma}^i\,, \tag{2.17}$$

where $\mathbb{1}$ is the identity matrix of size $2^{\frac{N-3}{2}}$. The non-zero spin connection is

$$\omega_{\theta_i} = \widetilde{\omega}_{\theta_i} - \frac{1}{2}\cos\theta_N \gamma^N \widetilde{\gamma}_{\theta_i}\,. \tag{2.18}$$

The eigenspinor equation is

$$\gamma^\mu \nabla_\mu \psi_\lambda = \left[\left(\partial_{\theta_N} + \frac{N-1}{2}\cot\theta_N\right)\gamma^N + \frac{1}{\sin\theta_N}\widetilde{\gamma}^{\theta_i}\widetilde{\nabla}_{\theta_i}\right]\psi_\lambda = i\lambda\psi_\lambda\,. \tag{2.19}$$

Choosing ψ_λ as

$$\psi_\lambda = \frac{1}{\sqrt{2}}\left(1 + i\gamma^N\right)A_\lambda(\theta_N)\widetilde{\psi}_\lambda + \frac{1}{\sqrt{2}}\left(1 - i\gamma^N\right)B_\lambda(\theta_N)\widetilde{\psi}_\lambda\,, \tag{2.20}$$

we find that we have the same relation between A_λ and B_λ as we had in Eq.(2.14). Hence the eigenvalues will be the same as those for the case of N even. We will now derive the eigenvalues for our spinor-vectors, as we have done in Ref.[29]

2.3 Eigenmodes of spinor-vectors on S^N

We denote the spinor-vectors as ψ_μ, where each of the components are spinors, for instance on S^3 we would write $\psi_\mu = (\psi_{\theta_1}, \psi_{\theta_2}, \psi_{\theta_3})$ where ψ_{θ_1}, ψ_{θ_2}, ψ_{θ_3} are spinors. To begin our investigation into spinor-vectors we find two orthogonal eigenspinor-vectors on S^2, which can be written as linear combinations of the basis $\gamma_\mu\psi_\lambda$ and $\nabla_\mu\psi_\lambda$, where ψ_λ is the eigenspinor on S^2. These are "non-Transverse and Traceless eigenmodes" (non-TT modes) as they do not satisfy the transverse and traceless conditions. These two eigenspinor-vectors can be generalised to the S^N case, and are analogous to the

longitudinal eigenmode for vector fields on spheres. These "non-TT eigenmodes" form a complete set of eigenmodes on S^2. For higher dimensional surfaces these modes do not represent a complete set and we must introduce TT eigenmodes. We are also required to consider the behaviour of the S^N spinor-vector components on S^{N-1}. Consider the surface S^3, we expect the following spinor-vector $\psi_{\theta_i} = (\psi_{\theta_1}, \psi_{\theta_2}, \psi_{\theta_3})$, with $\psi_{\theta_1}, \psi_{\theta_2}$ and ψ_{θ_3} representing spinors. Furthermore on S^3 we expect our "TT components", ψ_{θ_1} and ψ_{θ_2}, to behave like spinor-vectors on S^2. Since S^2 only has "non-TT eigenmodes" we should represent ψ_{θ_1} and ψ_{θ_2} as linear combinations of "non-TT eigenmodes" on S^3. As such ψ_{θ_3} acts like a spinor on S^2 and we represent it using a linear combination of spinor eigenmodes on S^2. This gives us our first type of "TT-eigenmode" which we can call the "TT-eigenmode I". The complete set of spinor-vectors on S^3 is therefore given by two "non-TT eigenmodes" and one "TT-eigenmode I". On S^4 spinors ψ_{θ_1}, ψ_{θ_2} and ψ_{θ_3} behave like spinor-vectors and ψ_{θ_4} behaves like a spinor on S^3. We therefore have two types of spinor-vectors on S^3, which we can be represent in two ways. Firstly we can represent ψ_{θ_1}, ψ_{θ_2} and ψ_{θ_3} as linear combination of "non-TT eigenmodes" on S^3, and ψ_{θ_4} represented with a linear combination of spinor eigenmodes on S^3, this is the "TT-eigenmode I" on S^4. Secondly we could represent ψ_{θ_1}, ψ_{θ_2} and ψ_{θ_3} as "TT-eigenmodes" on S^3 this means that ψ_{θ_4} must be zero, this is the "TT eigenmode II". Hence the complete set of eigenmodes on S^4 is given by two "non-TT eigenmodes", one "TT eigenmode I" and one "TT eigenmode II". Generally eigenmodes on S^N are represented by two "non-TT eigenmodes", one "TT-eigenmode I" and $N-3$ "TT-eigenmode II" where $N > 2$.

2.4 Spinor-vector non-TT eigenmodes on S^N

The Dirac eigenspinor-vector equation is

$$\gamma^\mu \nabla_\mu \psi_\nu = i\xi \psi_\nu \,, \tag{2.21}$$

where ξ is the eigenvalue for our non-TT eigenmode spinor-vectors. We construct eigenspinor-vectors on S^N using the linear combination

$$\psi_\nu = \nabla_\nu \psi_\lambda + a\gamma_\nu \psi_\lambda \,, \tag{2.22}$$

where ψ_λ is an eigenspinor on S^N and a is some constant. Plugging Eq.(2.22) into Eq.(2.21) we have

$$\begin{aligned} i\xi\psi_\nu =&\gamma^\mu\nabla_\mu\psi_\nu \\ =&\gamma^\mu\nabla_\mu(\nabla_\nu\psi_\lambda + a\gamma_\nu\psi_\lambda) \\ =&\gamma^\mu[\nabla_\mu,\nabla_\nu]\psi_\nu + \nabla_\nu(\gamma^\mu\nabla_\mu\psi_\lambda) + a\{\gamma^\mu,\gamma_\nu\}\nabla_\mu\psi_\lambda - a\gamma_\nu(\gamma^\mu\nabla_\mu\psi_\lambda)\,. \end{aligned} \tag{2.23}$$

The commutator can be rewritten in terms of the Riemann curvature tensor $R_{\mu\nu}{}^{\sigma\rho}$ as,

$$\begin{aligned} \gamma^\mu[\nabla_\mu,\nabla_\nu]\psi_\lambda =&\frac{1}{8}R_{\mu\nu}{}^{\sigma\rho}[\gamma_\sigma,\gamma_\rho]\psi_\lambda \\ =&\frac{1}{8}\gamma^\mu(\delta^\sigma_\mu\delta^\rho_\nu - \delta^\rho_\mu\delta^\sigma_\nu)[\gamma_\sigma,\gamma_\rho]\psi_\lambda \\ =&\frac{1}{4}\gamma^\mu[\gamma_\mu,\gamma_\nu]\psi_\lambda \\ =&\frac{1}{2}(N-1)\gamma_\nu\psi_\lambda\,. \end{aligned} \tag{2.24}$$

Then Eq.(2.23) becomes

$$\gamma^\mu\nabla_\mu\psi_\nu = (i\lambda+2a)\left(\nabla_\nu\psi_\lambda + \frac{-i\lambda+\frac{1}{2}(N-1)}{i\lambda+2a}\gamma_\nu\psi_\lambda\right)\,, \tag{2.25}$$

where $i\lambda$ is the spinor eigenvalue on S^N. Using Eq.(2.22) we can show that

$$a = \frac{1}{2}\left(-i\lambda \pm \sqrt{(N-1)-\lambda^2}\right)\,, \tag{2.26}$$

with non-TT eigenvalues

$$i\xi = i\lambda + 2a = \pm i\sqrt{\lambda^2-(N-1)}\,, \tag{2.27}$$

and non-TT mode eigenspinor-vectors as

$$\begin{aligned} \psi^{(1)}_\nu =&\nabla_\nu\psi_\lambda + \frac{1}{2}\left(-i\lambda+\sqrt{(N-1)-\lambda^2}\right)\gamma_\nu\psi_\lambda, \\ \psi^{(2)}_\nu =&\nabla_\nu\psi_\lambda + \frac{1}{2}\left(-i\lambda-\sqrt{(N-1)-\lambda^2}\right)\gamma_\nu\psi_\lambda\,. \end{aligned} \tag{2.28}$$

2.5 Spinor-vector TT eigenmode I on S^N

Here we denote the eigenvalues as $i\zeta$, to distinguish them from the non-TT eigenmodes. So our spinor equation with Dirac operator is

$$\gamma^\mu\nabla_\mu\psi_\nu = i\zeta\psi_\nu\,. \tag{2.29}$$

The transverse traceless condition is as follows,

$$\nabla^\mu \psi_\mu = \gamma^\mu \psi_\mu = 0 \,. \tag{2.30}$$

As we have done with the spinor eigenmodes in Sec.2.2, we will separate out the S^{N-1} part and we will have to separately consider the N odd case and the N even case.

2.5.1 N odd

Using Eq.(2.17) and Eq.(2.7) we find that Eq.(2.30) becomes

$$\begin{aligned} \gamma^\mu \psi_\mu = 0 \implies \gamma^{\theta_N} \psi_{\theta_N} =& \gamma^{\theta_i} \psi_{\theta_i} \,, \\ \psi_{\theta_N} =& -\frac{1}{\sin\theta_N} \gamma^N \widetilde{\gamma}^{\theta_i} \psi_{\theta_i} \,. \end{aligned} \tag{2.31}$$

Using the Christoffel symbols used in Eq.(2.2), Eq.(2.30) and Eq.(2.29) become

$$\nabla^\mu \psi_\mu = 0 \implies \left(\partial_{\theta_N} + \left(N - \frac{1}{2}\right)\cot\theta_N\right)\psi_{\theta_N} = -\frac{1}{\sin^2\theta_N}\widetilde{\nabla}^{\theta_i}\psi_{\theta_i} \,, \tag{2.32}$$

$$\gamma^\mu \nabla_\mu \psi_{\theta_N} = i\zeta\psi_{\theta_N} \implies \gamma^N \left(\partial_{\theta_N} + \left(\frac{N+1}{2}\right)\cot\theta_N\right)\psi_{\theta_N} + \frac{1}{\sin\theta_N}\widetilde{\gamma}^{\theta_i}\widetilde{\nabla}_{\theta_i}\psi_{\theta_N} = i\zeta\psi_{\theta_N} \,, \tag{2.33}$$

$$\begin{aligned} \gamma^\mu \nabla_\mu \psi_{\theta_i} = i\zeta\psi_{\theta_i} \implies & \gamma^N \left(\partial_{\theta_N} + \left(\frac{N-1}{2}\right)\cot\theta_N\right)\psi_{\theta_i} + 2\cot\theta_N \gamma^N \widetilde{\Sigma}^{\theta_j}_{\theta_i}\psi_{\theta_j} \\ & + \frac{1}{\sin\theta_N}\widetilde{\gamma}^{\theta_j}\widetilde{\nabla}_{\theta_j}\psi_{\theta_i} = i\zeta\psi_{\theta_i} \,. \end{aligned} \tag{2.34}$$

ψ_{θ_N} behaves like a spinor and we write them as linear combinations of the eigenspinors on S^{N-1}. The ψ_{θ_i} behave like a spinor-vector and we write them in terms of "non-TT eigenmode" spinor-vector on S^{N-1},

$$\psi_{\theta_N} = \frac{1}{\sqrt{2}}(1 + i\gamma^N)A^{(1)}\widetilde{\psi}_\lambda + \frac{1}{\sqrt{2}}(1 - i\gamma^N)A^{(2)}\widetilde{\psi}_\lambda \,, \tag{2.35}$$

$$\psi_{\theta_i} = \frac{1}{\sqrt{2}}(1 + i\gamma^N)(C^{(1)}\widetilde{\nabla}_{\theta_i}\widetilde{\psi}_\lambda + D^{(1)}\widetilde{\gamma}_{\theta_i}\widetilde{\psi}_\lambda) + \frac{1}{\sqrt{2}}(1 - i\gamma^N)\left(C^{(2)}\widetilde{\nabla}_{\theta_i}\widetilde{\psi}_\lambda + D^{(2)}\widetilde{\gamma}_{\theta_i}\widetilde{\psi}_\lambda\right) \,. \tag{2.36}$$

The coefficients $A^{(1,2)}, C^{(1,2)}$ and $B^{(1,2)}$ are functions of θ_N only and $\widetilde{\psi}_\lambda$ is the spinor eigenmode on S^{N-1}. Using these two definitions we can rewrite Eqs.(2.31) to (2.34) as follows

$$\pm\frac{i}{\sin\theta_N}\left(i\widetilde{\lambda}C^{(1,2)} + (N-1)D^{(1,2)}\right) = A^{(1,2)} \,, \tag{2.37}$$

$$-\frac{1}{\sin^2\theta_N}\left(\left[-\widetilde{\lambda}^2 + \frac{1}{4}(N-1)(N-2)\right]C^{(1,2)} + i\widetilde{\lambda}D^{(1,2)}\right) = \left(\partial_{\theta_N} + \left(N - \frac{1}{2}\right)\cot\theta_N\right)A^{(1,2)} \,, \tag{2.38}$$

$$\left(\partial_{\theta_N}+\left(\frac{N+1}{2}\right)\cot\theta_N\pm\frac{\widetilde{\lambda}}{\sin\theta_N}\right)A^{(1,2)}=\pm\zeta A^{(2,1)}\,, \tag{2.39}$$

$$\left(\partial_{\theta}+\left(\frac{N-3}{2}\right)\cot\theta_N\pm\frac{\widetilde{\lambda}}{\sin\theta_N}\right)D^{(1,2)}\mp\left(\frac{2}{\sin\theta_N}\right)D^{(1,2)}=\pm\zeta C^{(2,1)}\,, \tag{2.40}$$

$$\left(\partial_{\theta_N}+\left(\frac{3N-5}{2}\right)\cot\theta_N\mp\frac{\widetilde{\lambda}}{\sin\theta_N}\right)D^{(1,2)}+\left(i\widetilde{\lambda}\cot\theta_N\mp i\frac{N-2}{2\sin\theta_N}C^{(1,2)}\right)=\pm\zeta D^{(2,1)}\,. \tag{2.41}$$

As this system of equations is over determined we can solve for $C^{(1,2)}$ and $D^{(1,2)}$ and rewrite them in terms of $A^{(1,2)}$, the results are

$$C^{(1,2)}=\frac{\sin\theta_N}{\widetilde{\lambda}^2-\frac{1}{4}(N-1)^2}\left(\frac{N-1}{2}\cos\theta_N\mp\widetilde{\lambda}\right)A^{(1,2)}\mp\frac{N-1}{N-2}\frac{\zeta\sin^2\theta_N}{\widetilde{\lambda}-\frac{1}{4}(N-1)^2}A^{(2,1)}\,, \tag{2.42}$$

$$D^{(1,2)}=-\frac{i\sin\theta_N}{\widetilde{\lambda}^2-\frac{1}{4}(N-1)^2}\left(\widetilde{\lambda}\cos\theta_N\mp\frac{N-1}{2}\right)A^{(1,2)}\pm\frac{i\zeta\widetilde{\lambda}\sin^2\theta_N}{(N-2)\left(\widetilde{\lambda}^2-\frac{1}{4}(N-1)^2\right)}A^{(2,1)}. \tag{2.43}$$

Setting $A^{(1,2)}=(\sin\theta_N)^{-\frac{N+1}{2}}\,\mathbb{A}^{(1,2)}$, Eq.(2.39) becomes

$$\mathbb{A}^{(1,2)}=\left(\sin\frac{\theta_N}{2}\right)^{\left|\frac{1}{2}\pm\widetilde{\lambda}\right|+\frac{1}{2}}\left(\cos\frac{\theta_N}{2}\right)^{\left|\frac{1}{2}\mp\widetilde{\lambda}\right|+\frac{1}{2}}P_n^{\left|\frac{1}{2}\pm\widetilde{\lambda}\right|,\left|\frac{1}{2}\mp\widetilde{\lambda}\right|}(\cos\theta_N)\,, \tag{2.44}$$

and

$$\zeta=\pm\left(n+\left|\widetilde{\lambda}\right|+\frac{1}{2}\right), \tag{2.45}$$

where $\left|\widetilde{\lambda}\right|=\widetilde{n}+(N-1)/2$, $\widetilde{n}=0,1,2,...$ and $n=0,1,2,....$ Eq.(2.45) can be rewritten as

$$\zeta=\pm\left(j+\frac{N-1}{2}\right),\ j=\frac{1}{2},\frac{3}{2},\frac{5}{2},\frac{7}{2},.... \tag{2.46}$$

As such we have determined the eigenvalue for our eigenspinor-vectors for N and $N\geq 3$.

2.5.2 N even

We use the gamma matrices and spin connections as given in Eq.(2.9) and Eq.(2.10) and set $\psi_\mu=(\psi_{\theta_i},\psi_{\theta_N})$, with

$$\psi_{\theta_N}=\begin{pmatrix}\psi^{(1)}_{\theta_N}\\ \psi^{(2)}_{\theta_N}\end{pmatrix}\,,\quad \psi_{\theta_i}=\begin{pmatrix}\psi^{(1)}_{\theta_i}\\ \psi^{(2)}_{\theta_i}\end{pmatrix}\,. \tag{2.47}$$

This allows us to rewrite Eq.(2.21) and Eq.(2.30) as

$$\gamma^\mu\psi_\mu=0\implies\psi^{(1,2)}_{\theta_N}=\pm\frac{i}{\sin\theta_N}\widetilde{\gamma}^{\theta_i}\psi^{(1,2)}_{\theta_i}, \tag{2.48}$$

$$\nabla^{\mu}\psi_{\mu}=0 \implies \left(\partial_{\theta_N}+\left(N-\frac{1}{2}\right)\cot\theta_N\right)\psi^{(1,2)}_{\theta_N}=-\frac{1}{\sin^2\theta_N}\widetilde{\nabla}^{\theta_i}\psi^{(1,2)}_{\theta_i}, \tag{2.49}$$

$$\gamma^{\mu}\nabla_{\mu}\psi_{\theta_N}=i\zeta\psi_{\theta_N} \implies \left(\partial_{\theta_N}+\left(\frac{N+1}{2}\right)\cot\theta_N\right)\psi^{(1,2)}_{\theta_N}\mp\frac{i}{\sin\theta_N}\widetilde{\gamma}^{\theta_i}\widetilde{\nabla}_{\theta_i}\psi^{(1,2)}_{\theta_N}=i\zeta\psi^{(2,1)}_{\theta_N}, \tag{2.50}$$

$$\begin{aligned}\gamma^{\mu}\nabla_{\mu}\psi_{\theta_i}=i\zeta\psi_{\theta_i} \implies &\left(\partial_{\theta_N}+\left(\frac{N-1}{2}\right)\cot\theta_N\right)\psi^{(1,2)}_{\theta_i}+2\cot\theta_N\widetilde{\Sigma}^{\theta_j}_{\theta_i}\psi^{(1,2)}_{\theta_j}\\ &\mp\frac{i}{\sin\theta_N}\widetilde{\gamma}^{\theta_j}\widetilde{\nabla}_{\theta_j}\psi^{(1,2)}_{\theta_i}=i\zeta\psi^{(2,1)}_{\theta_i}.\end{aligned} \tag{2.51}$$

We set

$$\begin{aligned}&\psi^{(1)}_{\theta_N}=A^{(1)}\widetilde{\psi}_{\lambda}\,;\quad \psi^{(2)}_{\theta_N}=iA^{(2)}\widetilde{\psi}_{\lambda}\,;\\ &\psi^{(1)}_{\theta_i}=C^{(1)}\widetilde{\nabla}_{\theta_i}\widetilde{\psi}_{\lambda}+D^{(1)}\widetilde{\gamma}_{\theta_i}\widetilde{\psi}_{\lambda}\,;\quad \psi^{(2)}_{\theta_i}=iC^{(2)}\widetilde{\theta}_i\widetilde{\psi}_{\lambda}+iD^{(1)}\widetilde{\gamma}_{\theta_i}\widetilde{\gamma}_{\lambda}\,.\end{aligned} \tag{2.52}$$

Substituting these into Eqs.(2.48) and (2.51), we have the same results as we did for the N odd case. That is, we find that the eigenvalues are the same as those for the N odd case. We note that this is true only for $N>2$ since, as discussed before, there are no TT eigenmodes for the surface S^2.

2.6 Spinor-vector TT-Modes II on S^N

As discussed earlier in this section "TT eigenmodes II" are only possible for $N\geq 4$. We start by letting the eigenspinor-vector $\psi_{\theta_N}=0$, and the "TT mode" eigenspinor-vector on S^{N-1} will still be an eigenspinor-vector on S^N with suitable coefficients.

2.6.1 N odd

Setting spinor-vector ψ_{θ_i} as

$$\psi_{\theta_i}=\left(\frac{1}{\sqrt{2}}B^{(1)}\left(1+i\gamma^N\right)+\frac{1}{\sqrt{2}}B^{(2)}\left(1-i\gamma^N\right)\right)\widetilde{\psi}_{\theta_i}\,, \tag{2.53}$$

where $B^{(1)}$ and $B^{(2)}$ are functions of θ_N only, and substituting into Eq.(2.34) we have

$$\left(\partial_{\theta_N}+\left(\frac{N-3}{2}\right)\cot\theta_N\pm\frac{\widetilde{\zeta}}{\sin\theta_N}\right)B^{(1,2)}=\pm B^{(2,1)}\,. \tag{2.54}$$

By setting $B^{(1,2)}=(\sin\theta_N)^{-\left(\frac{N-3}{2}\right)}\mathbb{B}^{(1,2)}$, $\mathbb{B}^{(1,2)}$ is solved using a Jacobi polynomial. We find that $\widetilde{\zeta}$ is the same as for the "TT mode I" and given as $\widetilde{\zeta}=j+\frac{N-2}{2}$. Such that the eigenvalues on "TT mode II" are

$$i\zeta=\pm i\left(j+\frac{N-1}{2}\right),\ j=\frac{1}{2},\frac{3}{2},\frac{5}{2},\ldots \tag{2.55}$$

2.6.2 N even

Setting

$$\psi^{(1)}_{\theta_i} = B^{(1)}\widetilde{\psi}_{\theta_i} \; ; \; \psi^{(2)}_{\theta_i} = iB^{(2)}\widetilde{\psi}_{\theta_i} \; , \tag{2.56}$$

and using Eqs.(2.48) to (2.51) we find that the eigenvalue is still given as Eq.(2.55). We now have a complete collection of eigenvalues and eigenfunctions for our spinor-vectors. In the next chapter we use these results to calculate the potential function for our spin-3/2 particles near N-dimensional black holes.

Chapter 3

Effective potential for N-dimensional Schwarzschild black holes

In this chapter we determine the effective potential felt by our spin-3/2 particles near an N-dimensional Schwarzschild black hole. In order to determine our potential function we must construct a radial equation for our particles, this equation takes the form of a Schrödinger equation. In order to construct the radial equation we begin by calculating the equations of motion for our particle. We then try to find a way of rewriting them as a Schrödinger like equation. In order to get these equations of motion we must describe our particle using the appropriate relativistic field equation. In the case of the spin-3/2 we use the Rarita-Schwinger equation, first introduced by William Rarita and Julian Schwinger in 1941 [30]. We present the massless form of the Rarita-Schwinger equation in the next section and setup the mathematics required to calculate our effective potentials in the N-dimensional space time. Then, using the eigenspinor-vector modes we've constructed in Ch.2 we calculate the potential for non-TT modes and TT modes of our spinor-vectors in Secs. 3.2 and 3.3.

3.1 Massless Rarita-Schwinger field for N-dimensions

The massless form of the Rarita-Schwinger equation is given as

$$\gamma^{\mu\nu\alpha}\nabla_\nu\psi_\alpha = 0\,, \tag{3.1}$$

where the anti-symmetric Dirac gamma product is given as

$$\gamma^{\mu\nu\alpha} = \gamma^{[\mu}\gamma^{\nu}\gamma^{\alpha]} = \gamma^{\mu}\gamma^{\nu}\gamma^{\alpha} - \gamma^{\mu}g^{\nu\alpha} + \gamma^{\nu}g^{\mu\alpha} - \gamma^{\alpha}g^{\mu\nu} \,. \tag{3.2}$$

We then define our metric as

$$ds^2 = -f(r)dt^2 + \frac{1}{f(r)}dr^2 + r^2 d\bar{\Omega}^2_{N-2} \,, \tag{3.3}$$

where $f(r) = 1 - (2M/r)^{N-3}$ and $d\bar{\Omega}_{N-2}$ is the metric for the $N-2$ sphere. We now denote terms from the $N-2$ sphere with over bars. We choose the following gamma matrices,

$$\begin{aligned} \gamma^0 = i\sigma^3 \otimes \mathbb{1} \quad &\implies \gamma^t = \frac{1}{\sqrt{f}}(i\sigma^3 \otimes \mathbb{1}) \,, \\ \gamma^i = \sigma^1 \otimes \bar{\gamma}^i \quad &\implies \gamma^{\theta_i} = \frac{1}{r}(\sigma^1 \otimes \bar{\gamma}^{\theta_i}) \,, \\ \gamma^{N-1} = \sigma^2 \otimes \mathbb{1} \quad &\implies \gamma^r = \sqrt{f}(\sigma^2 \otimes \mathbb{1}) \,, \end{aligned} \tag{3.4}$$

with $\mathbb{1}$ being the $2^{\left(\frac{N}{2}\right)}$ unit matrix for the case of N even, and the $2^{\left(\frac{N-1}{2}\right)}$ unit matrix for the case of N odd. σ^i $[i = 1, 2, 3]$ are the Pauli matrices and $\bar{\gamma}^{\theta_i}$ are the gamma matrices for the $N-2$ sphere. The non-zero Christoffel symbols are

$$\begin{aligned} \Gamma^t_{tr} = \Gamma^t_{rt} = \frac{f'}{2f} \,, \quad \Gamma^r_{tt} = \frac{ff'}{2} \,, \quad \Gamma^r_{rr} = -\frac{f'}{2f} \,, \\ \Gamma^r_{\theta_i\theta_i} = -rf\bar{g}_{\theta_i\theta_i} \,, \quad \Gamma^{\theta_i}_{r\theta_i} = \Gamma^{\theta_i}_{\theta_i r} = \frac{1}{r} \,, \quad \Gamma^{\theta_i}_{\theta_j\theta_k} = \bar{\Gamma}^{\theta_i}_{\theta_j\theta_k} \,. \end{aligned} \tag{3.5}$$

With the following non-zero spin connections

$$\begin{aligned} \omega_t &= -\frac{f'}{4}(\sigma^1 \otimes \mathbb{1}) \,, \\ \omega_{\theta_i} &= \mathbb{1} \otimes \bar{\omega}_{\theta_i} + \frac{\sqrt{f}}{2}(i\sigma^3 \otimes \bar{\gamma}_{\theta_i}) \,. \end{aligned} \tag{3.6}$$

Finally our non-zero triple gamma products are given as

$$\begin{aligned} \gamma^{t\theta_i r} &= -\frac{1}{r}\left(\mathbb{1} \otimes \bar{\gamma}^{\theta_i}\right) \,, & \gamma^{t\theta_i\theta_j} &= \frac{1}{r^2\sqrt{f(r)}}\left(i\sigma^3 \otimes \bar{\gamma}^{\theta_i\theta_j}\right) \,, \\ \gamma^{r\theta_i\theta_j} &= \frac{\sqrt{f(r)}}{r^2}\left(\sigma^2 \otimes \bar{\gamma}^{\theta_i\theta_j}\right) \,, & \gamma^{\theta_i\theta_j\theta_k} &= \frac{1}{r^3}\left(\sigma^1 \otimes \bar{\gamma}^{\theta_i\theta_j\theta_k}\right) \,, \end{aligned} \tag{3.7}$$

where $\gamma^{\theta_i\theta_j} = \gamma^{\theta_i}\gamma^{\theta_j} - g^{\theta_i\theta_j}$ is the antisymmetric product of two gamma matrices.

3.1.1 Gamma matrices

In order to calculate our equations of motion we will require the results of summations across gamma matrices, covariant derivatives and the antisymmetric gamma matrix product on S^{N-2}. Some of these results are not obtained by trivial calculation so we present all relevant interactions and results in this section. We begin by looking at single contractions that return scalar like results

$$\bar{\gamma}^{\theta_i}\bar{\gamma}_{\theta_i}\bar{\psi}_\lambda = (N-2)\,\bar{\psi}_\lambda\,; \quad \bar{\gamma}^{\theta_i}\bar{\nabla}_{\theta_i} = i\bar{\lambda}\bar{\psi}_\lambda\,. \tag{3.8}$$

The contraction over $\bar{\nabla}^{\theta_i}\bar{\nabla}_{\theta_i}$ is more complicated,

$$\begin{aligned}
\bar{\gamma}^{\theta_i}\bar{\gamma}^{\theta_j}\bar{\nabla}_{\theta_j}\bar{\nabla}_{\theta_i}\bar{\psi}_\lambda &= -\bar{\lambda}^2\bar{\psi}_\lambda \\
&= \bar{\nabla}^{\theta_i}\bar{\nabla}_{\theta_i}\bar{\psi}_\lambda + \frac{1}{2}\bar{\gamma}^{\theta_i}\bar{\gamma}^{\theta_j}\left(\frac{1}{8}\bar{R}_{\theta_i\theta_j\theta_m\theta_n}\left[\bar{\gamma}^{\theta_m},\bar{\gamma}^{\theta_n}\right]\right)\bar{\psi}_\lambda \\
&= \bar{\nabla}^{\theta_i}\bar{\nabla}_{\theta_i}\bar{\psi}_\lambda - \frac{1}{4}(D-2)(D-3)\bar{\psi}_\lambda\,, \\
\therefore \bar{\nabla}^{\theta_i}\bar{\nabla}_{\theta_i}\bar{\psi}_\lambda &= \left(-\bar{\lambda}^2 + \frac{1}{4}(D-2)(D-3)\right)\bar{\psi}_\lambda\,.
\end{aligned} \tag{3.9}$$

Next we consider double contractions resulting in scalar like terms,

$$\begin{aligned}
\bar{\gamma}^{\theta_i\theta_j}\bar{\gamma}_{\theta_i}\bar{\nabla}_{\theta_j}\bar{\psi}_\lambda &= \frac{1}{2}\{\bar{\gamma}^{\theta_i},\bar{\gamma}^{\theta_j}\}\bar{\gamma}_{\theta_i}\bar{\nabla}_{\theta_j}\bar{\psi}_\lambda - \bar{\gamma}^{\theta_j}\bar{\gamma}^{\theta_i}\bar{\gamma}_{\theta_i}\bar{\nabla}_{\theta_j}\bar{\psi}_\lambda \\
&= \bar{\gamma}^{\theta_j}\bar{\nabla}_{\theta_j}\bar{\psi}_\lambda - (N-2)\bar{\gamma}^{\theta_i}\bar{\nabla}_{\theta_j}\bar{\psi}_\lambda \\
&= -\,(N-3)\,(i\bar{\lambda})\bar{\psi}_\lambda = -\bar{\gamma}^{\theta_i\theta_j}\bar{\nabla}_{\theta_i}\bar{\gamma}_{\theta_j}\bar{\psi}_\lambda\,,
\end{aligned} \tag{3.10}$$

$$\begin{aligned}
\bar{\gamma}^{\theta_i\theta_j}\bar{\nabla}_{\theta_i}\bar{\nabla}_{\theta_j}\bar{\psi}_\lambda &= \bar{\gamma}^{\theta_i}\bar{\nabla}_{\theta_i}\bar{\gamma}^{\theta_j}\bar{\nabla}_{\theta_j} - \bar{\nabla}^{\theta_i}\bar{\nabla}_{\theta_i}\bar{\psi}_\lambda \\
&= -\frac{1}{4}\,(N-2)\,(N-3)\,\bar{\psi}_\lambda\,,
\end{aligned} \tag{3.11}$$

$$\begin{aligned}
\bar{\gamma}^{\theta_i\theta_j}\bar{\gamma}_{\theta_i}\bar{\gamma}_{\theta_j}\bar{\psi}_\lambda &= -\left(\bar{\gamma}^{\theta_j}\bar{\gamma}^{\theta_i}\bar{\gamma}_{\theta_i}\bar{\gamma}_{\theta_j}\bar{\psi}_\lambda - \bar{\gamma}^{\theta_i}\bar{\gamma}_{\theta_i}\bar{\psi}_\lambda\right) \\
&= -(N-2)(N-3)\bar{\psi}_\lambda\,.
\end{aligned} \tag{3.12}$$

Next we consider single contractions resulting in vector like results

$$\bar{\gamma}^{\theta_i\theta_j}\bar{\nabla}_{\theta_j}\bar{\psi}_\lambda = i\bar{\lambda}\bar{\gamma}^{\theta_i}\bar{\psi}_\lambda - \bar{\nabla}^{\theta_i}\bar{\psi}_\lambda\,, \tag{3.13}$$

$$\bar{\gamma}^{\theta_i\theta_j}\bar{\gamma}_{\theta_j}\bar{\psi}_\lambda = (N-3)\bar{\gamma}^{\theta_i}\bar{\psi}_\lambda\,. \tag{3.14}$$

Finally we consider our triple gamma product vector components with two contractions

$$\begin{aligned}\bar{\gamma}^{\theta_i\theta_j\theta_k}\bar{\nabla}_{\theta_j}\bar{\nabla}_{\theta_k}\bar{\psi}_\lambda =& -\frac{1}{4}(N-4)(N-3)\bar{\gamma}^{\theta_i}\bar{\psi}_\lambda = -\bar{\gamma}^{\theta_i\theta_j\theta_k}\bar{\nabla}_{\theta_k}\bar{\nabla}_{\theta_j}\bar{\psi}_\lambda \,,\\ \bar{\gamma}^{\theta_i\theta_j\theta_k}\bar{\nabla}_{\theta_j}\bar{\gamma}_{\theta_k}\bar{\psi}_\lambda =& (N-4)\left(i\bar{\lambda}\bar{\gamma}^{\theta_i}\bar{\psi}_\lambda - \bar{\nabla}^{\theta_i}\bar{\psi}_\lambda\right) = -\bar{\gamma}^{\theta_i\theta_j\theta_k}\bar{\gamma}_{\theta_j}\bar{\nabla}_{\theta_k}\bar{\psi}_\lambda \,,\\ \bar{\gamma}^{\theta_i\theta_j\theta_k}\bar{\gamma}_{\theta_j}\bar{\gamma}_{\theta_k}\bar{\psi}_\lambda =& -(N-3)(N-4)\bar{\gamma}^{\theta_i}\bar{\psi}_\lambda = -\bar{\gamma}^{\theta_i\theta_j\theta_k}\bar{\gamma}_{\theta_k}\bar{\gamma}_{\theta_j}\bar{\psi}_\lambda \,.\end{aligned} \tag{3.15}$$

We now have everything that we require in order to calculate the effective potential for our spin-3/2 particles.

3.2 Non-TT spinor-vectors in Schwarzschild space times

We represent our radial, temporal and angular components of our particles as ψ_r, ψ_t and ψ_{θ_i}. The radial and temporal parts will behave as spinors on S^{N-2} and we write them as

$$\psi_r = \phi_r \otimes \bar{\psi}_\lambda \quad \text{and} \quad \psi_t = \phi_t \otimes \bar{\psi}_\lambda \,, \tag{3.16}$$

were $\bar{\psi}_\lambda$ is an eigenspinor on the S^{N-2}, with eigenvalues $i\bar{\lambda}$. The angular part, however, will behave as a spinor-vector on S^{N-2} and is given in Eq.(2.28). It is, however, more convenient to write it as

$$\psi_{\theta_i} = \phi^{(1)}_\theta \otimes \bar{\nabla}_{\theta_i}\bar{\psi}_\lambda + \phi^{(2)}_\theta \otimes \bar{\gamma}_{\theta_i}\bar{\psi}_\lambda \,, \tag{3.17}$$

where $\phi^{(1)}_\theta$, $\phi^{(2)}_\theta$ are functions of r and t which behave like 2-spinors. This is the same form as we have used for spinors when studying the 4-dimensional space time [31]. Using Eq.(3.1) we will derive our equations of motion and then try to rewrite them as Schrödinger like equations. We will initially work in the Weyl gauge, where $\phi_t = 0$, to determine our equations of motion and will then find a gauge invariant form.

3.2.1 Equations of motion

Firstly consider the case where $\mu = t$ in Eq.(3.1),

$$\begin{aligned}&\gamma^{t\nu\alpha}\nabla_\nu\psi_\alpha = 0\\ \implies 0 =& \gamma^{t\theta_i r}\left(\partial_{\theta_i}\psi_r + \omega_{\theta_i}\psi_r - \partial_r\psi_{\theta_i}\right) + \gamma^{t\theta_i\theta_j}\left(\partial_{\theta_i}\psi_{\theta_i} + \omega_{\theta_i}\psi_{\theta_i}\right) \,.\end{aligned} \tag{3.18}$$

By using the results from Eq.(3.16), Eq.(3.17) and Eqs.(3.8) to (3.15) this expands to

$$\begin{aligned}0 =&\Bigg(-\frac{i\bar{\lambda}}{r}\phi_r - (N-2)\frac{\sqrt{f(r)}}{2r}\left(i\sigma^3\right)\phi_r + \frac{i\bar{\lambda}}{r}\partial_r\phi_\theta^{(1)} - \frac{1}{4}\frac{(N-2)\,(N-3)}{r^2\sqrt{f(r)}}\left(i\sigma^3\right)\phi_\theta^{(1)} \\ &+ (N-3)\frac{i\bar{\lambda}}{2r^2}\phi_\theta^{(1)} + \frac{N-2}{r}\partial_r\phi_\theta^{(2)} + \frac{(N-2)(N-3)}{2r^2}\phi_\theta^{(2)} + (N-3)\frac{i\bar{\lambda}}{r^2\sqrt{f(r)}}\left(i\sigma^3\right)\phi_\theta^{(2)}\Bigg)\otimes\bar{\psi}_\lambda\,.\end{aligned} \tag{3.19}$$

Giving us our first equation of motion in terms of ϕ_r, $\phi_\theta^{(1)}$ and $\phi_\theta^{(2)}$

$$\begin{aligned}0 =& -\left[i\bar{\lambda} + \frac{\sqrt{f(r)}}{2}(N-2)(i\sigma^3)\right]\phi_r + \left[i\bar{\lambda}\partial_r - \frac{1}{4}\frac{(N-2)\,(N-3)}{r\sqrt{f(r)}}(i\sigma^3) + (N-3)\frac{i\bar{\lambda}}{2r}\right]\phi_\theta^{(1)} \\ &+ \left[(N-2)\partial_r + \frac{i\bar{\lambda}(N-3)}{r\sqrt{f(r)}}(i\sigma^3) + \frac{(N-2)(N-3)}{2r}\right]\phi_\theta^{(2)}\,.\end{aligned} \tag{3.20}$$

Next consider the case where $\mu = r$ in Eq.(3.1),

$$\begin{aligned}&\gamma^{r\nu\alpha}\nabla_\nu\psi_\alpha = 0 \\ \implies 0 =&\gamma^{r\theta_i t}\left(-\partial_t\psi_{\theta_i} - \omega_t\psi_{\theta_i}\right) + \gamma^{r\theta_i\theta_j}\left(\partial_{\theta_i}\psi_{\theta_j} + \omega_{\theta_i}\psi_{\theta_j}\right)\,.\end{aligned} \tag{3.21}$$

Again using the results from Eq.(3.16), Eq.(3.17) and Eqs.(3.8) to (3.15) this expands to

$$\begin{aligned}0 =&\Bigg(-\frac{i\bar{\lambda}}{r}\partial_t\phi_\theta^{(1)} + \frac{i\bar{\lambda}f'(r)}{4r}\left(\sigma^1\right)\phi_\theta^{(1)} + (N-3)\frac{i\lambda f(r)}{2r^2}\left(\sigma^1\right)\phi_\theta^{(1)} \\ &- (N-3)(N-2)\frac{\sqrt{f(r)}}{4r^2}\left(\sigma^2\right)\phi_\theta^{(1)} - \frac{N-2}{r}\partial_t\phi_\theta^{(2)} + (N-3)\frac{i\lambda\sqrt{f(r)}}{r^2}\left(\sigma^2\right)\phi_\theta^{(2)} \\ &+ (N-2)\frac{f'(r)}{4r}\left(\sigma^1\right)\phi_\theta^{(2)} + (N-2)(N-3)\frac{f(r)}{2r^2}\left(\sigma^1\right)\phi_\theta^{(2)}\Bigg)\otimes\bar{\psi}_\lambda\,.\end{aligned} \tag{3.22}$$

Giving us our second equation of motion

$$\begin{aligned}0 =& \left[-\frac{i\lambda}{\sqrt{f(r)}}\partial_t + \frac{i\lambda f'(r)}{4\sqrt{f(r)}}(\sigma^1) - \frac{(N-3)(N-2)}{4r}\sigma^2 + (N-3)\frac{i\lambda\sqrt{f(r)}}{2r}(\sigma^1)\right]\phi_\theta^{(1)} \\ &+ \left[-\frac{N-2}{\sqrt{f(r)}}\partial_t + (N-2)\frac{f'(r)}{4\sqrt{f(r)}}(\sigma^1) + (N-3)\frac{i\lambda}{r}(\sigma^2) + (N-2)(N-3)\frac{\sqrt{f(r)}}{2r}\sigma^1\right]\phi_\theta^{(2)}\,.\end{aligned} \tag{3.23}$$

Finally for $\mu = \theta_i$,

$$\begin{aligned}&\gamma^{\theta_i\nu\alpha}\nabla_\nu\psi_\alpha = 0 \\ \implies 0 =&\gamma^{\theta_i tr}\left(\partial_t\psi_r + \omega_t\psi_r\right) + \gamma^{\theta_i t\theta_j}\left(\partial_t\psi_{\theta_j} + \omega_t\psi_{\theta_j}\right) + \gamma^{\theta_i\theta_j r}\left(\partial_{\theta_j}\psi_r + \omega_{\theta_j}\psi_r - \partial_r\psi_{\theta_j}\right) \\ &+ \gamma^{\theta_i\theta_j\theta_k}\left(\partial_{\theta_j}\psi_{\theta_k} + \omega_{\theta_j}\psi_{\theta_k}\right)\,.\end{aligned} \tag{3.24}$$

Using the same approach as we have done for the previous two cases this expands to

$$
\begin{aligned}
0 =& \Bigg[-\frac{\sqrt{f(r)}}{r}\left(\sigma^2\right)\phi_r + \Bigg(\frac{1}{r\sqrt{f(r)}}(i\sigma^3)\partial_t + \frac{f'(r)}{4r\sqrt{f(r)}}\sigma^2 + \frac{\sqrt{f(r)}}{r}\sigma^2\partial_r \\
&+ \frac{\sqrt{f(r)}}{2r^2}(N-4)\sigma^2\Bigg)\phi_\theta^{(1)} - \frac{N-4}{r^2}\sigma^1\phi_\theta^{(2)}\Bigg] \otimes \bar{\nabla}^{\theta_i}\bar{\psi}_\lambda \\
&+ \Bigg[\Bigg(\partial_t - \frac{f'(r)}{4}\sigma^1 + \frac{i\bar{\lambda}\sqrt{f(r)}}{r}\sigma^2 - \frac{(N-3)f(r)}{2r}\sigma^1\Bigg)\phi_r \\
&+ \Bigg(-\frac{i\bar{\lambda}}{r\sqrt{f(r)}}(i\sigma^3)\partial_t - \frac{(i\bar{\lambda})f'(r)}{4r\sqrt{f(r)}}\sigma^2 - \frac{(i\bar{\lambda})\sqrt{f(r)}}{r}\sigma^2\partial_r - \frac{(N-3)\,(N-4)}{4r^2}\sigma^1 \\
&- (N-4)\frac{(i\bar{\lambda})\sqrt{f(r)}}{2r^2}\Bigg)\phi_\theta^{(1)} + \Bigg(-\frac{N-3}{r\sqrt{f(r)}}(i\sigma^3)\partial_t - (N-3)\frac{f'(r)}{4r\sqrt{f(r)}}\sigma^2 \\
&- (N-3)\frac{\sqrt{f(r)}}{r}\sigma^2\partial_r + (N-4)\frac{(i\bar{\lambda})}{r^2}\sigma^1 - (N-3)(N-4)\frac{\sqrt{f(r)}}{2r^2}\sigma^2\Bigg)\phi_\theta^{(2)}\Bigg] \otimes \bar{\gamma}^{\theta_i}\bar{\psi}_\lambda\,.
\end{aligned}
\tag{3.25}
$$

Giving us our final two equations of motion,

$$
\begin{aligned}
0 =& \Bigg(\frac{1}{r\sqrt{f(r)}}(i\sigma^3)\partial_t + \frac{\sqrt{f(r)}}{r}\sigma^2\partial_r + \frac{f'(r)}{4r\sqrt{f(r)}}\sigma^2 \\
&+ (N-4)\frac{\sqrt{f(r)}}{2r^2}\sigma^2\Bigg)\phi_\theta^{(1)} - \left(\frac{N-4}{r^2}\sigma^1\right)\phi_\theta^{(2)} - \left(\frac{\sqrt{f(r)}}{r}\sigma^2\right)\phi_r\,,
\end{aligned}
\tag{3.26}
$$

and

$$
\begin{aligned}
0 =& -\Bigg(\frac{i\bar{\lambda}}{r\sqrt{f(r)}}(i\sigma^3)\partial_t + \frac{i\bar{\lambda}\sqrt{f(r)}}{r}\sigma^2\partial_r + \frac{i\bar{\lambda}f'(r)}{4r\sqrt{f(r)}}\sigma^2 + (N-3)\,(N-4)\,\frac{1}{4r^2}\sigma^1 \\
&+ (N-4)\frac{i\bar{\lambda}\sqrt{f(r)}}{2r^2}\Bigg)\phi_\theta^{(1)} - \Bigg(\frac{N-3}{r\sqrt{f(r)}}(i\sigma^3)\partial_t + (N-3)\frac{\sqrt{f(r)}}{r}\sigma^2\partial_r + (N-3)\frac{f'(r)}{4r\sqrt{f(r)}}\sigma^2 \\
&- (N-4)\frac{i\bar{\lambda}}{r^2}\sigma^1 + (N-3)\,(N-4)\,\frac{\sqrt{f(r)}}{2r^2}\Bigg)\phi_\theta^{(2)} + \Bigg(\partial_t - \frac{(N-3)f(r)}{2r}\sigma^1 \\
&- \frac{f'(r)}{4}\sigma^1 + \frac{i\bar{\lambda}\sqrt{f(r)}}{r}\sigma^2\Bigg)\phi_r\,.
\end{aligned}
\tag{3.27}
$$

We now have our four equations of motion, Eqs.(3.20), (3.23), (3.26) and (3.27), in terms of ϕ_r, $\phi_\theta^{(1)}$ and $\phi_\theta^{(2)}$. The functions ϕ_r, $\phi_\theta^{(1)}$ and $\phi_\theta^{(2)}$ are, however, not gauge invariant. In the next section we investigate this gauge variance and determine the appropriate transformations in order to create our gauge invariant radial equation.

3.2.2 Gauge-invariant variable

If we consider a system where only gravitational forces are present then

$$\gamma^{\mu\nu\alpha}\nabla_\nu\nabla_\alpha\varphi = \frac{1}{8}\gamma^{\mu\nu\alpha}R_{\nu\alpha\rho\sigma}\gamma^\rho\gamma^\sigma\varphi\,. \tag{3.28}$$

This allows our spinors to transform as

$$\psi'_\mu = \psi_\mu + \nabla_\mu\varphi\,, \tag{3.29}$$

and still possess the correct symmetry as given in Eq.(3.1). This is not the case if our metric is charged and we would need to introduce terms containing the electromagnetic field strength. We can simplify the expression given in Eq.(3.28) by exploiting the symmetry of the Riemann tensor,

$$\begin{aligned}\gamma^\mu\gamma^\nu\gamma^\alpha\left(R_{\mu\nu\alpha\beta}+R_{\nu\alpha\mu\beta}+R_{\alpha\mu\nu\beta}\right)=0 \implies 3\left(\gamma^\mu\gamma^\nu\gamma^\alpha R_{\mu\nu\alpha\beta}+2\gamma^\alpha R_{\alpha\beta}\right)=0\,,\\ \implies \gamma^\mu\gamma^\nu\gamma^\alpha R_{\mu\nu\alpha\beta}=-2\gamma^\alpha R_{\alpha\beta}\,.\end{aligned} \tag{3.30}$$

We also have that

$$\gamma^\mu\gamma^\nu\gamma^\alpha\gamma^\beta R_{\mu\nu\alpha\beta} = -2R\,. \tag{3.31}$$

Using these two identities Eq.(3.28) becomes

$$\begin{aligned}\frac{1}{8}\gamma^{\mu\nu\alpha}R_{\nu\alpha\rho\sigma}\gamma^\rho\gamma^\sigma &= \frac{1}{8}\left(\gamma^\mu\gamma^\nu\gamma^\sigma-\gamma^\mu g^{\nu\sigma}+\gamma^\nu g^{\mu\sigma}-\gamma^\sigma g^{\mu\nu}\right)\gamma^\rho\gamma^\sigma R_{\nu\alpha\rho\sigma}\\ &= \frac{1}{4}\left(2\gamma^\alpha R^\mu_\alpha-\gamma^\mu R\right)\varphi\,.\end{aligned} \tag{3.32}$$

This is zero for Ricci flat space times like the N-dimensional Schwarzschild space time. However for de Sitter and anti-de Sitter space times it does not vanish, so we would need to modify the covariant derivative in those cases in order to respect the gauge symmetry. This means we can perform the above transformation on our spinors. Firstly consider the transformation of ϕ_r and ϕ_t. Take $\varphi = \phi\otimes\bar{\psi}_\lambda$ then Eq.(3.29) becomes

$$\begin{aligned}\psi'_t = \psi_t + \nabla_t\psi \implies \phi'_t = \phi_t + \partial_r\phi - \frac{f'(r)}{4}\sigma^1\phi\,,\\ \psi'_r = \psi_r + \nabla_r\psi \implies \phi'_r = \phi_r + \partial_r\phi\,.\end{aligned} \tag{3.33}$$

Next consider the transformation of our angular components of ψ_μ. They are given as

$$\begin{aligned}
&\psi'_{\theta_i} = \psi_{\theta_i} + \nabla_{\theta_i}\varphi\,, \\
\Longrightarrow\ &\phi_\theta^{'(1)} \otimes \bar{\nabla}_{\theta_i}\bar{\psi}_\lambda + \phi_\theta^{'(2)} \otimes \bar{\gamma}_{\theta_i}\bar{\psi}_\lambda = \left(\phi_\theta^{(1)} + \phi\right) \otimes \bar{\nabla}_{\theta_i}\bar{\psi}_\lambda + \left(\phi_\theta^{(2)} + \frac{\sqrt{f(r)}}{2}(i\sigma^3)\phi\right) \otimes \bar{\gamma}_{\theta_i}\bar{\psi}_\lambda\,, \\
\Longrightarrow\ &\phi_\theta^{'(1)} = \phi_\theta^{(1)} + \phi\,; \quad \phi_\theta^{'(2)} = \phi_\theta^{(2)} + \frac{\sqrt{f(r)}}{2}(i\sigma^3)\phi\,.
\end{aligned} \tag{3.34}$$

So clearly ϕ_t, ϕ_r, $\phi_\theta^{(1)}$ and $\phi_\theta^{(2)}$ are not gauge invariant. We need to perform a transformation of these spinors in order to obtain gauge invariant functions, where we use the transformation we have used for the 4-dimensional space time [31]

$$\Phi = -\frac{\sqrt{f}}{2}(i\sigma^3)\phi_\theta^{(1)} + \phi_\theta^{(2)}\,. \tag{3.35}$$

Note that we have assumed that there is no dimensional dependence for our gauge invariant variable.

3.2.3 Non-TT potential

Using the gauge-invariant variable Φ, Eq.(3.20), Eq.(3.23) and Eq.(3.26) become

$$\begin{aligned}
&\left((N-2)\partial_r + (N-3)\frac{i\bar{\lambda}}{r\sqrt{f}}(i\sigma^3) + \frac{(N-2)(N-3)}{2r}\right)\Phi \\
&\qquad + \left(i\bar{\lambda} + \frac{N-2}{2}\sqrt{f}i\sigma^3\right)\partial_r\phi_\theta^{(1)} = \left(i\bar{\lambda} + \frac{N-2}{2}\sqrt{f}(i\sigma^3)\right)\phi_r\,,
\end{aligned} \tag{3.36}$$

$$\begin{aligned}
&\left(-\frac{N-2}{\sqrt{f}}\partial_t + \frac{(N-2)(N-3)\sqrt{f}}{2r}\sigma^1 + \frac{(N-2)f'}{4\sqrt{f}}\sigma^1 + (N-3)\frac{i\bar{\lambda}}{r}\sigma^2\right)\Phi \\
&\qquad + \left(-\left(\frac{i\bar{\lambda}}{\sqrt{f}} + \frac{N-2}{2}i\sigma^3\right)\partial_t + \frac{i\bar{\lambda}f'}{4\sqrt{f}}\sigma^1 - \frac{N-2}{8}f'\sigma^2\right)\phi_\theta^{(1)} = 0\,,
\end{aligned} \tag{3.37}$$

and

$$\left(\frac{1}{\sqrt{f}}(i\sigma^3)\partial_t + \sqrt{f}\sigma^2\partial_r + \frac{f'}{4\sqrt{f}}\sigma^2\right)\phi_\theta^{(1)} - \left(\frac{N-4}{r}\sigma^1\right)\Phi - \sqrt{f}\sigma^2\phi_r = 0\,. \tag{3.38}$$

We have used that $f' = (N-3)(1-f)/r$ to simplify our equations. We can now use Eq.(3.36), Eq.(3.37) and Eq.(3.38) to derive a gauge invariant equation of motion in

terms of only Φ,

$$\begin{aligned}
&\left(\frac{N-2}{2}\sqrt{f}+\bar{\lambda}\sigma^3\right)\left[-(N-2)\sigma^1\partial_t+\frac{N-2}{4}f'+\frac{N-3}{r}\sqrt{f}\left(\frac{N-2}{2}\sqrt{f}-\bar{\lambda}\sigma^3\right)\right]\Phi\\
&=\left(\frac{N-2}{2}\sqrt{f}-\bar{\lambda}\sigma^3\right)\left[(N-2)f\partial_r+\frac{N-3}{r}\sqrt{f}\left(\frac{N-2}{2}\sqrt{f}-\bar{\lambda}\sigma^3\right)\right]\Phi\\
&\quad+\left(\frac{N-2}{2}\sqrt{f}-\bar{\lambda}\sigma^3\right)\left[\frac{N-4}{r}\sqrt{f}\left(\frac{N-2}{2}\sqrt{f}+\bar{\lambda}\sigma^3\right)\right]\Phi\,.
\end{aligned} \tag{3.39}$$

Component wise Φ is given as

$$\Phi=\begin{pmatrix}\Phi_1(r)e^{-i\omega t}\\ \Phi_2(r)e^{-i\omega t}\end{pmatrix}\,. \tag{3.40}$$

Eq.(3.39) then becomes

$$\left(\frac{B}{A}\right)f\partial_r\phi_1-\frac{f'}{4}\phi_1-2\left(\frac{B}{A}\right)\frac{N-3}{N-2}\frac{\sqrt{f}\bar{\lambda}}{r}\phi_1+\frac{N-4}{N-2}\frac{\sqrt{f}}{r}B\phi_1=i\omega\phi_2\,, \tag{3.41}$$

$$\left(\frac{A}{B}\right)f\partial_r\phi_2-\frac{f'}{4}\phi_2+2\left(\frac{A}{B}\right)\frac{N-3}{N-2}\frac{\sqrt{f}\bar{\lambda}}{r}\phi_1+\frac{N-4}{N-2}\frac{\sqrt{f}}{r}A\phi_2=i\omega\phi_1\,, \tag{3.42}$$

where we have set

$$A=\frac{N-2}{2}\sqrt{f}+\bar{\lambda}\,,\quad B=\frac{N-2}{2}\sqrt{f}-\bar{\lambda}\,. \tag{3.43}$$

We can further simplify the above equation by defining

$$\widetilde{\Phi}_1=r^{\frac{N-4}{2}}\left(\frac{f^{1/4}}{\frac{N-2}{2}\sqrt{f}+\bar{\lambda}}\right)\Phi_1\,;\quad \widetilde{\Phi}_2=r^{\frac{N-4}{2}}\left(\frac{f^{1/4}}{\frac{N-2}{2}\sqrt{f}-\bar{\lambda}}\right)\Phi_2\,. \tag{3.44}$$

Eq.(3.41) and Eq.(3.42) then becomes

$$\left(\frac{d}{dr_*}-W\right)\widetilde{\Phi}_1=i\omega\widetilde{\Phi}_2\,;\quad \left(\frac{d}{dr_*}+W\right)\widetilde{\Phi}_2=i\omega\widetilde{\Phi}_1\,, \tag{3.45}$$

where r_* is the tortoise coordinate and is defined as $d/dr_*=fd/dr$. W is a supersymmetric like potential and is determined to be

$$W=\frac{|\bar{\lambda}|\sqrt{f}}{r}\left(\frac{\left(\frac{2}{N-2}\right)^2|\bar{\lambda}|^2-1-\frac{N-4}{N-2}\left(\frac{2M}{r}\right)^{N-3}}{\left(\frac{2}{N-2}\right)^2|\bar{\lambda}|^2-f}\right)\,. \tag{3.46}$$

This allows us to write our Schrödinger like equation to describe our particles, where we have called this equation our radial equation, given as

$$-\frac{d^2}{dr_*^2}\widetilde{\Phi}_1 + V_1\widetilde{\Phi}_1 = \omega^2\widetilde{\Phi}_1\,; \quad -\frac{d^2}{dr_*^2}\widetilde{\Phi}_2 + V_2\widetilde{\Phi}_2 = \omega^2\widetilde{\Phi}_2\,, \tag{3.47}$$

with isospectral potentials

$$V_{1,2} = \pm f\frac{dW}{dr} + W^2\,, \tag{3.48}$$

where $f = 1-(\frac{2M}{r})^{N-3}$ in N-dimensional space. As $\bar{\lambda} = n+(N-2)/2$ and $n = 0, 1, 2, ...$, we rewrite it as $\bar{\lambda} = j + \frac{N-3}{2}$, where $j = \frac{1}{2}, \frac{3}{2}, \frac{5}{2}, ...$ So Eq.(3.46) becomes

$$W = \frac{\left(j+\frac{N-3}{2}\right)\sqrt{f}}{r}\left(\frac{\left(\frac{2}{N-2}\right)^2\left(j-\frac{1}{2}\right)\left(j+\frac{2N-5}{2}\right) - \frac{N-4}{N-2}\left(\frac{2M}{r}\right)^{N-3}}{\left(\frac{2}{N-2}\right)^2\left(j-\frac{1}{2}\right)\left(j+\frac{2N-5}{2}\right) + \left(\frac{2M}{r}\right)^{N-3}}\right)\,. \tag{3.49}$$

$V(r)$ is then explicitly given as

$$\begin{aligned} V_{(1,2)} =& \frac{X\sqrt{f}(j+\frac{N-3}{2}}{r^2(X+Y)^2}\left[X\left(\left(j+\frac{N-3}{2}\right)\sqrt{f} \pm \left(\frac{N-1}{2}\right)Y \mp 1\right) \mp \left(\frac{2N^2-13N+19}{N-2}\right)Y^2\right] \\ &+ \frac{X\sqrt{f}\left(j+\frac{N-3}{2}\right)}{r^2\left(X+Y\right)^2}\left[\pm 2(D-4)Y\right] \\ &+ \frac{(j+\frac{N-3}{2})\sqrt{f}Y^2}{r^2\left(X+Y\right)^2}\left(\frac{N-4}{N-2}\right)\left[\left(j+\frac{N-3}{2}\right)\left(\frac{N-4}{N-2}\right)\sqrt{f} \pm 1 \mp \left(\frac{N-1}{2}\right)Y\right]. \end{aligned} \tag{3.50}$$

$$X = \left(\frac{2}{N-2}\right)^2\left(j-\frac{1}{2}\right)\left(j+\frac{2N-5}{2}\right)\,,\quad Y = \left(\frac{2M}{r}\right)^{N-3}. \tag{3.51}$$

Setting $N = 4$ we find that our potential is the same as we have obtained previously [31]

$$\begin{aligned} V_{1,2} =& \frac{\left(j-\frac{1}{2}\right)\left(j+\frac{1}{2}\right)\left(j+\frac{3}{2}\right)\sqrt{f}}{r^2(\left(j-\frac{1}{2}\right)\left(j+\frac{3}{2}\right)+\left(\frac{2M}{r}\right))^2} \\ &\times\left[\mp\frac{2M^2}{r^2} + \left(j-\frac{1}{2}\right)\left(j+\frac{3}{2}\right)\left(\left(j+\frac{1}{2}\right)\sqrt{f} \pm \left(\frac{3M}{r}\right) \mp 1\right)\right]. \end{aligned} \tag{3.52}$$

3.3 TT spinor-vectors in Schwarzschild space times

3.3.1 Equations of motion

We set the radial and temporal parts of the spin-3/2 field, ψ_r and ψ_t, for the spinor-vector as those for the spinor, given in Eq.(3.16). The angular part, ϕ_{θ_i}, can be written in terms of the TT mode eigenspinor-vector on S^N as

$$\phi_{\theta_i} = \phi_\theta \otimes \bar{\psi}_{\theta_i}\,, \tag{3.53}$$

where $\bar{\psi}_{\theta_i}$ is the TT mode eigenspinor-vector which includes the "TT mode I" and "TT mode II", and ψ_θ behaves like a 2-spinor. As we have done for the spinors we will use the Weyl gauge and first look at the case where $\mu = t$ in Eq.(3.1),

$$\begin{aligned} &\gamma^{t\nu\alpha}\nabla_\nu\psi_\alpha = 0 \\ \Longrightarrow\ &-\sqrt{f}\left(i\bar{\lambda} + \frac{N-2}{2}\sqrt{f}i\sigma^3\right)\phi_r \otimes \bar{\psi}_\lambda + \frac{1}{r}i\sigma^3\phi_\theta \otimes \bar{\nabla}^{\theta_i}\bar{\psi}_{\theta_i} \\ &\quad + \left(\sqrt{f}\partial_r - \frac{i\bar{\zeta}}{r}i\sigma^3 + \frac{N-3}{2r}\sqrt{f}\right)\phi_\theta \otimes \bar{\gamma}^{\theta_i}\bar{\psi}_{\theta_i} = 0\,. \end{aligned} \tag{3.54}$$

Note that $i\bar{\lambda}$ is the eigenvalue of the spinor eigenmode on the $N-2$ sphere, and $i\bar{\zeta}$ is the eigenvalue of the TT spinor-vector eigenmode on the $N-2$ sphere. For the case of $\mu = r$, we have

$$\begin{aligned} &\gamma^{r\nu\alpha}\nabla_\nu\psi_\alpha = 0 \\ \Longrightarrow\ &\frac{1}{r}\sigma^2\phi_\theta \otimes \bar{\nabla}^{\theta_i}\bar{\psi}_{\theta_i} + \left(-\frac{1}{\sqrt{f}}\partial_t - \frac{i\bar{\zeta}}{r}\sigma^2 + \frac{\sqrt{f}}{2}\left(\frac{f'}{2f} + \frac{N-3}{r}\right)\sigma^1\right)\phi_\theta \otimes \bar{\gamma}^{\theta_i}\bar{\psi}_{\theta_i} = 0\,. \end{aligned} \tag{3.55}$$

Finally for $\mu = \theta_i$, we have

$$\begin{aligned} &\gamma^{\theta_i\nu\alpha}\nabla_\nu\psi_\alpha = 0 \\ \Longrightarrow\ &-\frac{\sqrt{f}}{r}\sigma^2\phi_r \otimes \bar{\nabla}^{\theta_i}\bar{\psi} + \left(\partial_t - \frac{f'}{4}\sigma^1 - \frac{N-3}{2r}f\sigma^1 + \frac{i\lambda}{r}\sqrt{f}\right)\phi_r \otimes \bar{\gamma}^{\theta_i}\bar{\psi} \\ &+\left(\frac{1}{r\sqrt{f}}i\sigma^3\partial_t + \frac{\sqrt{f}}{r}\sigma^2\partial_r + \frac{f'}{4r\sqrt{f}}\sigma^2 + \frac{N-4}{2r^2}\sqrt{f}\sigma^2 + \frac{i\bar{\zeta}}{r^2}\sigma^1\right)\phi_\theta \otimes \left(\bar{\psi}^{\theta_i} - \bar{\gamma}^{\theta_i}\left(\bar{\gamma}^{\theta_j}\bar{\psi}_{\theta_j}\right)\right) \\ &-\frac{1}{r^2}\sigma^1\phi_\theta \otimes \left(\bar{\nabla}^{\theta_i}\left(\bar{\gamma}^{\theta_j}\bar{\psi}_{\theta_j}\right) - \bar{\gamma}^{\theta_i}\left(\bar{\nabla}^{\theta_j}\bar{\psi}_{\theta_j}\right)\right) = 0\,. \end{aligned} \tag{3.56}$$

Applying the TT conditions on a sphere, namely $\bar{\gamma}^{\theta_i}\bar{\psi}_{\theta_i} = \bar{\nabla}^{\theta_i}\bar{\psi}_{\theta_i} = 0$, Eq.(3.54) leads to $\phi_r = 0$. Using Eq.(3.56) we find that the equation of motion for the spinor-vector is

$$\left(i\sigma^3\partial_t + f\sigma^2\partial_r + \frac{f'}{4}\sigma^2 + \frac{N-4}{2r}f\sigma^2\frac{\sqrt{f}}{r}i\bar{\zeta}\sigma^1\right)\phi_\theta = 0\,. \tag{3.57}$$

In this case ψ_θ is gauge invariant, so we directly derive the radial equation in the next section.

3.3.2 TT potential

Assuming ϕ_θ is given as

$$\phi_\theta = \sigma^2 e^{-i\omega t}\begin{pmatrix}\Phi_{\theta_1}\\ \Phi_{\theta_2}\end{pmatrix}\,, \tag{3.58}$$

Eq.(3.57) can then be rewritten as

$$\begin{aligned}\left(f\partial_r+\frac{f'}{4}+\frac{N-4}{2r}f-\frac{\sqrt{f}}{r}\bar{\zeta}\right)\Phi_{\theta_1}&=i\omega\Phi_{\theta_2}\,,\\ \left(f\partial_r+\frac{f'}{4}+\frac{N-4}{2r}f+\frac{\sqrt{f}}{r}\bar{\zeta}\right)\Phi_{\theta_2}&=i\omega\Phi_{\theta_1}\,.\end{aligned}\tag{3.59}$$

These expressions can be simplified using the following transformations,

$$\bar{\Phi}_{\theta_1}=r^{\frac{N-4}{2}}f^{\frac{1}{4}}\Phi_{\theta_1}\quad\text{and}\quad\bar{\Phi}_{\theta_2}=r^{\frac{N-4}{2}}f^{\frac{1}{4}}\Phi_{\theta_2}\,.\tag{3.60}$$

This allows us to rewrite Eqs.(3.59) as

$$\begin{aligned}\left(f\partial_r-\frac{\sqrt{f}}{r}\bar{\zeta}\right)\bar{\Phi}_{\theta_1}&=i\omega\bar{\Phi}_{\theta_2}\,,\\ \left(f\partial_r+\frac{\sqrt{f}}{r}\bar{\zeta}\right)\bar{\Phi}_{\theta_2}&=i\omega\bar{\Phi}_{\theta_1}\,,\end{aligned}\tag{3.61}$$

with radial equations

$$-\frac{d^2}{dr_*^2}\bar{\Phi}_{\theta_1}+\mathbb{V}_1\bar{\Phi}_{\theta_1}=\omega^2\bar{\Phi}_{\theta_1}\,;\quad-\frac{d^2}{dr_*^2}\bar{\Phi}_{\theta_2}+\mathbb{V}_2\bar{\Phi}_{\theta_2}=\omega^2\bar{\Phi}_{\theta_2}\,,\tag{3.62}$$

where

$$\mathbb{V}_{1,2}=\pm f\frac{d\mathbb{W}}{dr}+\mathbb{W}^2\,,\tag{3.63}$$

and

$$\mathbb{W}=\frac{\sqrt{f}}{r}\bar{\zeta}\,.\tag{3.64}$$

As $\bar{\zeta}=n+\frac{N-2}{2}$ and $n=0,1,2,...$ we rewrite $\bar{\zeta}=j+\frac{N-3}{2}$ where $j=\frac{1}{2},\frac{3}{2},\frac{5}{2},....$ Our spinor-vector potentials are then explicitly given as

$$\begin{aligned}\mathbb{V}_{1,2}=&\pm\frac{\sqrt{1-\left(\frac{2M}{r}\right)^{N-3}}}{r^2}\left(j+\frac{N-3}{2}\right)\\ &\times\left[\frac{N-1}{2}\left(\frac{2M}{r}\right)-1\pm\sqrt{1-\left(\frac{2M}{r}\right)^{N-3}}\left(j+\frac{N-3}{2}\right)\right].\end{aligned}\tag{3.65}$$

This is the same potential as obtained in Ref.[32] where the radial equation of a spin-1/2 field on the N-dimensional Schwarzschild black hole space time is considered. We can then say that the radial equation for the gravitino field is equivalent to that of the spinor field when the eigenmode on S^N is the "TT mode", with $\psi_t=\psi_r=0$, and only ψ_{θ_i} remains. We therefore have two types of potentials, one relating to non-TT eigenmodes, Eq.(3.48), and the other relating to our TT eigenmodes, Eq.(3.65). Kodama and Ishibashi have suggested that when studying small perturbations $h_{\mu\nu}=\delta g_{\mu\nu}$ of the

maximally symmetric space, $g_{\mu\nu}$, then we can group the perturbations into three distinct groups namely:"Tensor variables", "Vector variables" and "Scalar variables" [33]. This occurs because the Einstein equations can be decomposed into three groups, namely "Tensor", "Vector" and "Scalar", and our maximally symmetric metric preserves this decomposition such that variables of each type only appear in their respective Einstein equations[34]. As such we can think of our perturbations as either "Tensor perturbations", "Vector perturbations" and "Scalar perturbations". In our case we can consider perturbations due to our TT eigenspinor-vectors to be spinor-vector perturbations, since the TT condition is $\nabla^{\mu}\psi_{\mu} = 0$, and our non-TT eigenspinor-vectors to be spinor perturbations [33]. We now refer to our non-TT potential as a spinor potential and the TT potential as a spinor-vector potential.

Chapter 4

Quasi normal modes

QNMs can be considered to be the characteristic sound of a black hole. As was made evident by the recent advanced LIGO results, where reproducing the detected QN frequency as a sound wave results in a "chirp" [35]. With higher dimensional theories predicting the creation of higher dimensional black holes at the LHC the study of QNMs may become a topic of increasing interest for high energy physics [14, 36]. In this chapter we use two methods to determine the numerical values of our QNMs. We will use the 3rd order WKB method, developed by Iyer and Will [23], and the 6th order WKB method developed by Kononplya [24]. Secondly we have used the Improved AIM which is developed in the following papers [26, 37–39]. A brief review of how these methods are used is given in the introduction.

4.1 WKB method

In order to use the WKB method we must rewrite Eqs.(3.47) and (3.62) as

$$\frac{d^2\psi}{dr^2} + Q(r)\psi = 0\,, \tag{4.1}$$

where $Q(x) = \omega^2 - V(x)$. Here ω represents the QNM and $V(x)$ represents the potential function. The boundary conditions of our QNMs leads to a constraint on our coefficients for our Taylor expansion of $Q(r)$. The 3rd order constraint is

$$\frac{iQ_0}{2Q_0''}^{\frac{1}{2}} - \Lambda_2 - \Lambda_3 = n + \frac{1}{2}\,, \tag{4.2}$$

and our 6th order constraint is

$$\frac{iQ_0}{2Q_0''}^{\frac{1}{2}} - \Lambda_2 - \Lambda_3 - \Lambda_4 - \Lambda_5 - \Lambda_6 = n + \frac{1}{2}\,. \tag{4.3}$$

The expressions for Λ_2, Λ_3, Λ_4, Λ_5 and Λ_6 are lengthy and are presented in Ref.[24]. We determine the QNMs by solving for ω in Eqs.(4.2) and (4.3).

4.2 Improved AIM

For the improved AIM we perform a change of variable on our radial coordinate, where Ref.[26] suggests $\xi^2 = 1-2M/r$ as a suitable variable change. This change in coordinates means we are now working on a compact space, since $0 < \xi \leq 1$. Using the boundary conditions of our QNMs we can write their wave equation as

$$\begin{aligned} \widetilde{\Phi} &\sim e^{i\omega r_*} \qquad \text{for } r_* \to \infty\,; \\ \widetilde{\Phi} &\sim e^{-i\omega r_*} \qquad \text{for } r_* \to -\infty\,. \end{aligned} \tag{4.4}$$

With r_* as the tortoise coordinate, where the general formula for an N-dimensional tortoise coordinate is given in Ref. [40]

$$r_* = r + \sum_{n=1}^{N-3} \frac{e^{2\pi i \frac{n}{N-3}}}{N-3} 2M \ln\left(r - 2Me^{2\pi i \frac{n}{N-3}}\right)\,. \tag{4.5}$$

Plugging Eq.(4.5) into our wave functions for our particles gives us our general behaviour of the particles for our N-dimensional space

$$\widetilde{\Phi} \sim e^{\pm\frac{2iM\omega}{1-\xi^2}} \prod_{n=1}^{N-3} \left(1 - \left(1-\xi^2\right)\Theta(n)\right)^{\pm\frac{2iM\omega\Theta(n)}{N-3}} \left[\left(1-\xi^2\right)\Theta(n)\right]^{\pm\frac{2iM\omega\Theta(n)}{N-3}}\,, \tag{4.6}$$

where $\Theta(n) = e^{\frac{2\pi i n}{N-3}}$. Clearly at the boundaries of our system, namely $\xi = 1, 0$, we would encounter asymptotic behaviour. We extract this asymptotic behaviours from $\widetilde{\Phi}$ and write

$$\widetilde{\Phi} = \beta(\xi)\chi(\xi)\,, \tag{4.7}$$

where $\beta(\xi)$ contains our asymptotic behaviours, and $\chi(\xi)$ satisfies the equation

$$\chi''(\xi) = \lambda_0\chi(\xi) + s_0\chi(\xi)\,. \tag{4.8}$$

The functions λ_0 and s_0 are determined to be

$$\lambda_0 = -\left(2\frac{\beta'(\xi)}{\beta(\xi)} + A\right) , \tag{4.9}$$

$$s_0 = -\left(\frac{\beta''(\xi)}{\beta(\xi)} + \frac{\beta'(\xi)}{\beta(\xi)}A + B\right) , \tag{4.10}$$

with

$$A = \frac{\xi''}{\xi'} + \frac{f'}{f} ; \quad B = \frac{1}{(f\xi')^2}\left(\omega^2 - V\right) . \tag{4.11}$$

We can then apply the improved AIM method as described in the introduction to Eq.(4.8) and determine the numerical values of our QNMs use 200 iterations of the improved AIM.

4.3 Spinor results

In this section we present the numerical values for our spinor perturbations on the N-dimensional Schwarzschild black hole. Tabulated results for our QNMs are presented in Tabs.4.1-4.6, a more graphical representation of these results are given in Fig.4.1.

TABLE 4.1: Low-lying ($n \leq l$, with $l = j - 3/2$ and $N = 4$) QNM frequencies using the WKB and the AIM methods for the spinor perturbation potential.

l	n	3rd order WKB	6th order WKB	AIM
0	0	0.3087-0.0902i	0.3113-0.0902i	0.3112-0.0902i
1	0	0.5295-0.0938i	0.5300-0.0938i	0.5300-0.0937i
1	1	0.5103-0.2858i	0.5114-0.2854i	0.5113-0.2854i
2	0	0.7346-0.0949i	0.7348-0.0949i	0.7347-0.0948i
2	1	0.7206-0.2870i	0.7210-0.2869i	0.7210-0.2869i
2	2	0.6960-0.4844i	0.6953-0.4855i	0.6952-0.4855i
3	0	0.9343-0.0954i	0.9344-0.0954i	0.9343-0.0953i
3	1	0.9233-0.2876i	0.9235-0.2876i	0.9235-0.2875i
3	2	0.9031-0.4834i	0.9026-0.4840i	0.9025-0.4839i
3	3	0.8759-0.6835i	0.8733-0.6870i	0.8732-0.6870i
4	0	1.1315-0.0956i	1.1315-0.0956i	1.1315-0.0956i
4	1	1.1224-0.2879i	1.1225-0.2879i	1.1225-0.2879i
4	2	1.1053-0.4828i	1.1050-0.4831i	1.1049-0.4830i
4	3	1.0817-0.6812i	1.0798-0.6830i	1.0798-0.6829i
4	4	1.0530-0.8828i	1.0485-0.8891i	1.0484-0.8890i
5	0	1.3273-0.0958i	1.3273-0.0958i	1.3273-0.0957i
5	1	1.3196-0.2881i	1.3196-0.2881i	1.3196-0.2881i
5	2	1.3048-0.4824i	1.3045-0.4826i	1.3045-0.4825i
5	3	1.2839-0.6795i	1.2826-0.6805i	1.2826-0.6805i
5	4	1.2582-0.8794i	1.2547-0.8832i	1.2547-0.8831i
5	5	1.2284-1.0821i	1.2221-1.0915i	1.2220-1.0914i

TABLE 4.2: Low-lying ($n \leq l$, with $l = j - 3/2$ and $N = 5$) QNM frequencies using the WKB and the AIM methods for the spinor perturbation potential.

l	n	3rd order WKB	6th order WKB	AIM
0	0	0.4409-0.1529i	0.4641-0.1436i	0.4641-0.1435i
1	0	0.7530-0.1653i	0.7558-0.1652i	0.7558-0.1651i
1	1	0.6902-0.5112i	0.6989-0.5075i	0.6988-0.5074i
2	0	1.0322-0.1700i	1.0332-0.1700i	1.0332-0.1700i
2	1	0.9869-0.5182i	0.9900-0.5172i	0.9899-0.5172i
2	2	0.9076-0.8835i	0.9070-0.8868i	0.9070-0.8868i
3	0	1.2998-0.1723i	1.3003-0.1723i	1.3003-0.1723i
3	1	1.2639-0.5221i	1.2654-0.5217i	1.2653-0.5216i
3	2	1.1985-0.8839i	1.1974-0.8858i	1.1974-0.8857i
3	3	1.1111-1.2586i	1.1009-1.2748i	1.1008-1.2748i
4	0	1.5617-0.1736i	1.5620-0.1736i	1.5619-0.1736i
4	1	1.5319-0.5244i	1.5327-0.5242i	1.5326-0.5242i
4	2	1.4761-0.8841i	1.4751-0.8852i	1.4750-0.8851i
4	3	1.3998-1.2546i	1.3919-1.2639i	1.3919-1.2638i
4	4	1.3070-1.6346i	1.2874-1.6672i	1.2873-1.6672i
5	0	1.8204-0.1744i	1.8205-0.1744i	1.8205-0.1744i
5	1	1.7947-0.5259i	1.7952-0.5258i	1.7951-0.5257i
5	2	1.7461-0.8842i	1.7453-0.8848i	1.7452-0.8848i
5	3	1.6783-1.2515i	1.6724-1.2571i	1.6723-1.2570i
5	4	1.5950-1.6274i	1.5793-1.6478i	1.5793-1.6478i
5	5	1.4983-2.0108i	1.4696-2.0621i	1.4695-2.0621i

TABLE 4.3: Low-lying ($n \leq l$, with $l = j - 3/2$ and $N = 6$) QNM frequencies using the WKB and the AIM methods for the spinor perturbation potential.

l	n	3rd order WKB	6th order WKB	AIM
0	0	0.5916-0.2260i	0.5714-0.2197i	0.5713-0.2197i
1	0	0.9479-0.2274i	0.9548-0.2229i	0.9547-0.2229i
1	1	0.8210-0.7101i	0.8416-0.6761i	0.8415-0.6761i
2	0	1.2745-0.2336i	1.2771-0.2329i	1.2771-0.2328i
2	1	1.1832-0.7155i	1.1934-0.7085i	1.1933-0.7084i
2	2	1.0199-1.2310i	1.0220-1.2203i	1.0220-1.2202i
3	0	1.5862-0.2376i	1.5874-0.2373i	1.5874-0.2373i
3	1	1.5140-0.7220i	1.5187-0.7198i	1.5187-0.7197i
3	2	1.3804-1.2296i	1.3803-1.2284i	1.3802-1.2283i
3	3	1.1990-1.7635i	1.1734-1.7885i	1.1734-1.7885i
4	0	1.8900-0.2400i	1.8906-0.2399i	1.8906-0.2399i
4	1	1.8298-0.7266i	1.8323-0.7257i	1.8323-0.7256i
4	2	1.7160-1.2302i	1.7152-1.2305i	1.7151-1.2304i
4	3	1.5584-1.7552i	1.5396-1.7714i	1.5396-1.7714i
4	4	1.3647-2.3005i	1.3099-2.3698i	1.3099-2.3698i
5	0	2.1890-0.2417i	2.1894-0.2416i	2.1894-0.2416i
5	1	2.1371-0.7299i	2.1387-0.7294i	2.1386-0.7293i
5	2	2.0378-1.2311i	2.0369-1.2315i	2.0368-1.2315i
5	3	1.8982-1.7499i	1.8841-1.7603i	1.8841-1.7603i
5	4	1.7246-2.2867i	1.6825-2.3309i	1.6825-2.3308i
5	5	1.5215-2.8396i	1.4372-2.9604i	1.4372-2.9604i

TABLE 4.4: Low-lying ($n \leq l$, with $l = j - 3/2$ and $N = 7$) QNM frequencies using the WKB and the AIM methods for the spinor perturbation potential.

l	n	3rd order WKB	6th order WKB	AIM
0	0	0.7725-0.2978i	0.7530-0.3037i	0.7008-0.3036i
1	0	1.1441-0.2893i	1.1415-0.2831i	1.1231-0.2976i
1	1	0.9465-0.9065i	0.9267-0.8783i	0.9266-0.8782i
2	0	1.4998-0.2921i	1.5026-0.2891i	1.5026-0.2891i
2	1	1.3503-0.8967i	1.3624-0.8752i	1.3623-0.8752i
2	2	1.0742-1.5569i	1.0498-1.5066i	1.0498-1.5065i
3	0	1.8419-0.2960i	1.8438-0.2949i	1.8438-0.2949i
3	1	1.7229-0.9007i	1.7323-0.8923i	1.7322-0.8922i
3	2	1.4961-1.5419i	1.4953-1.5198i	1.4953-1.5198i
3	3	1.1835-2.2325i	1.1146-2.2262i	1.1146-2.2261i
4	0	2.1755-0.2991i	2.1766-0.2986i	2.1765-0.2986i
4	1	2.0760-0.9061i	2.0818-0.9025i	2.0817-0.9024i
4	2	1.8838-1.5389i	1.8845-1.5300i	1.8845-1.5300i
4	3	1.6124-2.2095i	1.5732-2.2118i	1.5731-2.2118i
4	4	1.2773-2.9207i	1.1449-2.9964i	1.1449-2.9964i
5	0	2.5035-0.3013i	2.5042-0.3011i	2.5041-0.3010i
5	1	2.4177-0.9105i	2.4213-0.9087i	2.4212-0.9087i
5	2	2.2504-1.5392i	2.2507-1.5351i	2.2506-1.5351i
5	3	2.0107-2.1974i	1.9842-2.2013i	1.9841-2.2013i
5	4	1.7101-2.8899i	1.6167-2.9406i	1.6166-2.9405i
5	5	1.3583-3.6159i	1.1548-3.7942i	1.1547-3.7941i

TABLE 4.5: Low-lying ($n \leq l$, with $l = j - 3/2$ and $N = 8$) QNM frequencies using the WKB and the AIM methods for the spinor perturbation potential.

l	n	3rd order WKB	6th order WKB	AIM
0	0	0.9675-0.3597i	0.9577-0.3647i	0.9675-0.3597i
1	0	1.3483-0.3498i	1.3372-0.3477i	1.3483-0.3498i
1	1	1.0776-1.0933i	1.0370-1.0848i	1.0775-1.0933i
2	0	1.7213-0.3485i	1.7199-0.3446i	1.7213-0.3484i
2	1	1.5065-1.0692i	1.5036-1.0437i	1.5064-1.0692i
2	2	1.0973-1.8731i	1.0016-1.8170i	1.0972-1.8730i
3	0	2.0845-0.3507i	2.0856-0.3484i	2.0844-0.3507i
3	1	1.9099-1.0665i	1.9192-1.0496i	1.9099-1.0664i
3	2	1.5665-1.8349i	1.5456-1.7789i	1.5665-1.8348i
3	3	1.0897-2.6898i	0.9046-2.6246i	1.0896-2.6897i
4	0	2.4398-0.3534i	2.4410-0.3522i	2.4398-0.3534i
4	1	2.2931-1.0700i	2.3017-1.0611i	2.2931-1.0699i
4	2	2.0011-1.8219i	2.0000-1.7896i	2.0010-1.8218i
4	3	1.5816-2.6380i	1.4930-2.5837i	1.5815-2.6380i
4	4	1.0674-3.5290i	0.7606-3.5381i	1.0674-3.5290i
5	0	2.7896-0.3558i	2.7904-0.3552i	2.7895-0.3557i
5	1	2.6627-1.0745i	2.6690-1.0698i	2.6627-1.0745i
5	2	2.4091-1.8186i	2.4114-1.8008i	2.4090-1.8185i
5	3	2.0378-2.6105i	1.9886-2.5773i	2.0377-2.6105i
5	4	1.5711-3.4654i	1.3755-3.4609i	1.5711-3.4653i
5	5	1.0321-4.3822i	0.5837-4.5299i	1.0321-4.3822i

TABLE 4.6: Low-lying ($n \leq l$, with $l = j - 3/2$ and $N = 9$) QNM frequencies using the WKB and the AIM methods for the spinor perturbation potential.

l	n	3rd order WKB	6th order WKB	AIM
0	0	1.1706-0.4149i	1.1654-0.4181i	1.1706-0.4148i
1	0	1.5593-0.4062i	1.5473-0.4069i	1.5593-0.4062i
1	1	1.2078-1.2636i	1.1700-1.2482i	1.2078-1.2635i
2	0	1.9438-0.4026i	1.9376-0.3998i	1.9437-0.4026i
2	1	1.6581-1.2319i	1.6427-1.2082i	1.6580-1.2318i
2	2	1.0963-2.1769i	0.9333-2.1004i	1.0962-2.1768i
3	0	2.3216-0.4029i	2.3202-0.4000i	2.3215-0.4028i
3	1	2.0850-1.2224i	2.0882-1.2003i	2.0849-1.2223i
3	2	1.6038-2.1138i	1.5438-2.0212i	1.6037-2.1137i
3	3	0.9361-3.1458i	0.5638-3.0044i	0.9361-3.1457i
4	0	2.6931-0.4046i	2.6934-0.4027i	2.6930-0.4046i
4	1	2.4923-1.2226i	2.5009-1.2076i	2.4922-1.2225i
4	2	2.0795-2.0861i	2.0671-2.0180i	2.0795-2.0861i
4	3	1.4794-3.0549i	1.2900-2.8966i	1.4793-3.0549i
4	4	0.7585-4.1483i	0.1237-4.0124i	0.7585-4.1482i
5	0	3.0595-0.4066i	3.0601-0.4055i	3.0594-0.4066i
5	1	2.8851-1.2260i	2.8934-1.2168i	2.8850-1.2259i
5	2	2.5261-2.0759i	2.5286-2.0323i	2.5260-2.0759i
5	3	1.9901-3.0021i	1.8953-2.8832i	1.9901-3.0020i
5	4	1.3222-4.0371i	0.9244-3.8754i	1.3222-4.0370i
5	5	0.5692-5.1717i	-0.3542-5.1389i	0.5691-5.1716i

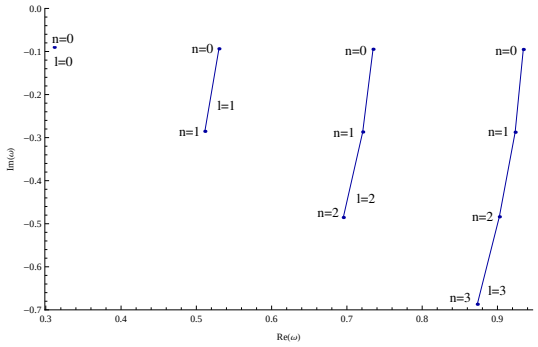

(A) QNMs associated to the 4-dimensional black hole for l=0 to l=3.

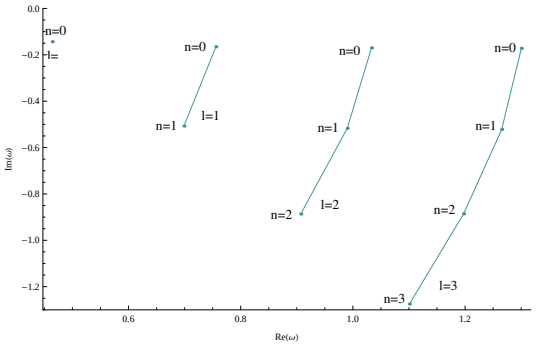

(B) QNMs associated to the 5-dimensional black hole for l=0 to l=3.

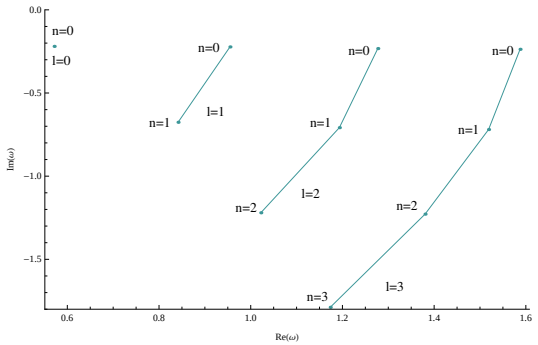

(C) QNMs associated to the 6-dimensional black hole for l=0 to l=3.

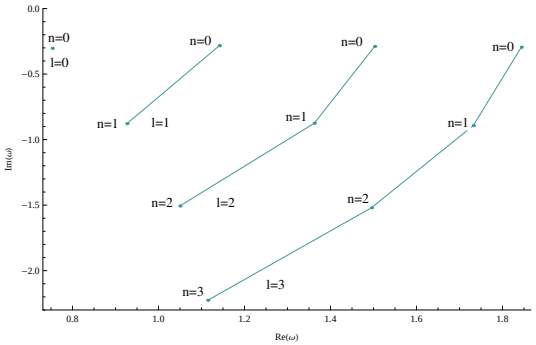

(D) QNMs associated to the 7-dimensional black hole for l=0 to l=3.

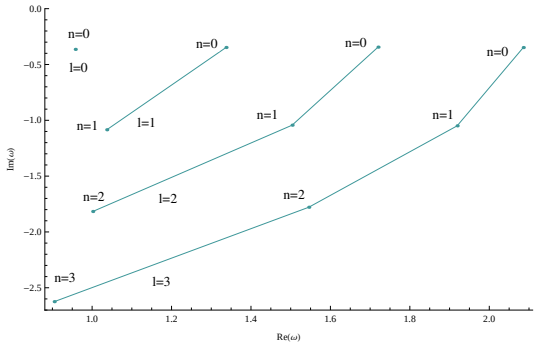

(E) QNMs associated to the 8-dimensional black hole for l=0 to l=3.

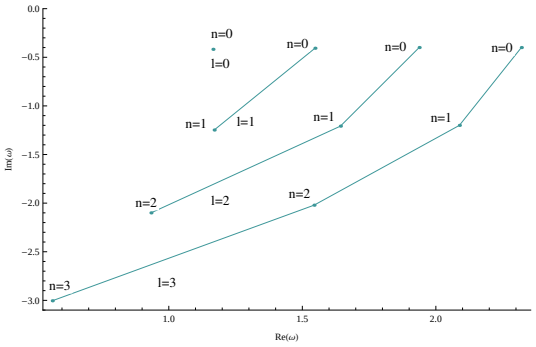

(F) QNMs associated to the 9-dimensional black hole for l=0 to l=3.

FIGURE 4.1: Low-lying ($n \leq l$, with $l = j - 3/2$ and $0 \leq l \leq 3$) gravitino QNM frequencies for spinor perturbations.

Our results obtained for the 4-dimensional space time agree with those obtained in Ref.[41] where they have used the Prony method to obtain their results. We clearly see that as the mode number n gets larger the real part decreases and the imaginary part increases. Since the imaginary part represents the damping part of our QNM this means that larger n modes are more unlikely to be detect compared to lower n modes. We also see that an increase in the number of dimensions results in an increase in both the real part and the damping part of our QNMs. This means that we would see higher energy

particles being emitted from our large dimensional black holes, but the short lifespan of these QNMs would make them difficult to detect. We should note that the 6th order WKB method returns erroneous results when $n = l$ in the 8- and 9-dimensional space times, this might be occurring due to non-convergence of our WKB method in these cases. It is suspected that this non-convergence occurs since the WKB series converges only asymptotically, and in these case we should rather use the results of the AIM.

4.4 Spinor-vector results

We have applied the same methods, namely the AIM and the WKB method, to the potential obtained for the eigenspinor-vectors, $\mathbb{V}_1$, given in Eq.(3.65). The analysis is very similar to that of the eigenspinors, however here we do not have QNMs for the spinor-vector in 4-dimensions as there exist no spinor vectors on a 2-sphere. We present the numerical results in Tabs.4.7 - 4.11 and a graphic presentation of the results is given in Fig.(4.2).

TABLE 4.7: Low-lying ($n \leq l$, with $l = j - 3/2$ and $N = 5$) QNM frequencies using the WKB and the AIM methods for the spinor-vector perturbation potential.

l	n	3rd order WKB	6th order WKB	AIM
0	0	0.6061-0.1769i	0.6127-0.1775i	0.3800-0.0963i
1	0	0.8639-0.1768i	0.8661-0.1771i	0.1240-0.6007i
1	1	0.8081-0.5444i	0.8141-0.5431i	0.2329-0.6715i
2	0	1.1171-0.1768i	1.1181-0.1769i	0.5978-0.3909i
2	1	1.0744-0.5383i	1.0771-0.5378i	0.7543-0.2909i
2	2	0.9998-0.9163i	0.9992-0.9204i	0.7297-0.4919i
3	0	1.3689-0.1768i	1.3693-0.1768i	0.9602-0.0962i
3	1	1.3342-0.5355i	1.3356-0.5352i	0.9497-0.2901i
3	2	1.2712-0.9060i	1.2702-0.9080i	0.9294-0.4881i
3	3	1.1872-1.2891i	1.1779-1.3050i	0.9010-0.6925i
4	0	1.6199-0.1768i	1.6202-0.1768i	1.1530-0.0962i
4	1	1.5908-0.5339i	1.5916-0.5338i	1.1442-0.2897i
4	2	1.5364-0.8999i	1.5355-0.9010i	1.1270-0.4860i
4	3	1.4622-1.2765i	1.4548-1.2856i	1.1024-0.6869i
4	4	1.3721-1.6625i	1.3536-1.6942i	1.0717-0.8938i
5	0	1.8707-0.1768i	1.8708-0.1768i	1.3457-0.0962i
5	1	1.8455-0.5330i	1.8460-0.5329i	1.3381-0.2894i
5	2	1.7978-0.8961i	1.7970-0.8967i	1.3233-0.4847i
5	3	1.7314-1.2680i	1.7257-1.2735i	1.3017-0.6834i
5	4	1.6498-1.6485i	1.6347-1.6684i	1.2743-0.8867i
5	5	1.5553-2.0363i	1.5277-2.0864i	1.2421-1.0957i

TABLE 4.8: Low-lying ($n \leq l$, with $l = j - 3/2$ and $N = 6$) QNM frequencies using the WKB and the AIM methods for the spinor-vector perturbation potential.

l	n	3rd order WKB	6th order WKB	AIM
0	0	0.8209-0.2453i	0.8343-0.2510i	0.6127-0.1774i
1	0	1.1205-0.2465i	1.1254-0.2483i	0.8660-0.1770i
1	1	1.0073-0.7667i	1.0252-0.7671i	0.8140-0.5431i
2	0	1.4120-0.2470i	1.4144-0.2473i	0.7836-0.7080i
2	1	1.3255-0.7559i	1.3343-0.7550i	0.9367-0.7509i
2	2	1.1725-1.2976i	1.1756-1.3054i	0.9991-0.9203i
3	0	1.7007-0.2471i	1.7019-0.2472i	1.0723-0.7455i
3	1	1.6305-0.7509i	1.6353-0.7500i	1.2086-0.7263i
3	2	1.5016-1.2777i	1.5021-1.2807i	1.2702-0.9080i
3	3	1.3276-1.8301i	1.3057-1.8640i	1.1778-1.3050i
4	0	1.9880-0.2472i	1.9887-0.2471i	1.6202-0.1768i
4	1	1.9289-0.7481i	1.9316-0.7475i	1.5915-0.5338i
4	2	1.8177-1.2661i	1.8173-1.2675i	1.5355-0.9010i
4	3	1.6642-1.8053i	1.6471-1.8241i	1.4547-1.2856i
4	4	1.4762-2.3641i	1.4257-2.4377i	1.3535-1.6942i
5	0	2.2748-0.2472i	2.2752-0.2471i	1.8708-0.1768i
5	1	2.2236-0.7464i	2.2252-0.7460i	1.8459-0.5329i
5	2	2.1258-1.2588i	2.1252-1.2596i	1.7970-0.8967i
5	3	1.9887-1.7886i	1.9755-1.8000i	1.7256-1.2734i
5	4	1.8187-2.3361i	1.7787-2.3820i	1.6346-1.6684i
5	5	1.6200-2.8993i	1.5401-3.0222i	1.5276-2.0864i

TABLE 4.9: (Low-lying ($n \leq l$, with $l = j - 3/2$ and $N = 7$) QNM frequencies using the WKB and the AIM methods for the spinor-vector perturbation potential.

l	n	3rd order WKB	6th order WKB	AIM
0	0	1.0317-0.3043i	1.0499-0.3229i	0.6014-1.2660i
1	0	1.3632-0.3081i	1.3706-0.3140i	1.1170-0.4979i
1	1	1.1731-0.9655i	1.2094-0.9788i	1.0252-0.7671i
2	0	1.6831-0.3096i	1.6877-0.3106i	1.4504-0.2985i
2	1	1.5386-0.9503i	1.5581-0.9515i	1.3343-0.7549i
2	2	1.2756-1.6458i	1.2888-1.6603i	1.1755-1.3054i
3	0	1.9985-0.3101i	2.0010-0.3101i	1.3891-0.8216i
3	1	1.8819-0.9436i	1.8931-0.9419i	1.5004-0.8251i
3	2	1.6620-1.6138i	1.6685-1.6152i	1.5021-1.2806i
3	3	1.3607-2.3310i	1.3188-2.3792i	1.3056-1.8639i
4	0	2.3118-0.3102i	2.3132-0.3101i	1.4838-1.0256i
4	1	2.2136-0.9399i	2.2203-0.9383i	1.7075-1.0313i
4	2	2.0250-1.5958i	2.0282-1.5946i	1.8173-1.2675i
4	3	1.7602-2.2887i	1.7287-2.3110i	1.6470-1.8241i
4	4	1.4338-3.0200i	1.3223-3.1346i	1.4257-2.4376i
5	0	2.6241-0.3102i	2.6249-0.3101i	1.8094-1.0509i
5	1	2.5390-0.9375i	2.5431-0.9365i	2.2252-0.7460i
5	2	2.3738-1.5846i	2.3753-1.5833i	2.1251-1.2595i
5	3	2.1380-2.2611i	2.1144-2.2727i	1.9754-1.7999i
5	4	1.8430-2.9708i	1.7573-3.0378i	1.7787-2.3820i
5	5	1.4978-3.7124i	1.3110-3.9189i	1.5401-3.0221i

TABLE 4.10: Low-lying ($n \leq l$, with $l = j - 3/2$ and $N = 8$) QNM frequencies using the WKB and the AIM methods for the spinor-vector perturbation potential.

l	n	3rd order WKB	6th order WKB	AIM
0	0	1.2409-0.3556i	1.2578-0.3978i	1.0498-0.3228i
1	0	1.5986-0.3631i	1.6063-0.3772i	1.3705-0.3140i
1	1	1.3104-1.1432i	1.3697-1.1940i	1.2093-0.9788i
2	0	1.9413-0.3663i	1.9484-0.3687i	1.6876-0.3106i
2	1	1.7240-1.1248i	1.7585-1.1358i	1.5581-0.9514i
2	2	1.3136-1.9682i	1.3480-2.0003i	1.2887-1.6603i
3	0	2.2775-0.3673i	2.2819-0.3673i	2.0009-0.3101i
3	1	2.1034-1.1175i	2.1254-1.1157i	1.8931-0.9419i
3	2	1.7637-1.9205i	1.7844-1.9179i	1.6685-1.6152i
3	3	1.2924-2.8068i	1.2265-2.8519i	1.3188-2.3791i
4	0	2.6108-0.3677i	2.6133-0.3673i	2.2257-0.5093i
4	1	2.4648-1.1135i	2.4783-1.1103i	2.2202-0.9383i
4	2	2.1759-1.8952i	2.1887-1.8855i	2.0282-1.5945i
4	3	1.7625-2.7389i	1.7138-2.7446i	1.7287-2.3110i
4	4	1.2546-3.6543i	1.0454-3.7724i	1.3223-3.1346i
5	0	2.9427-0.3677i	2.9441-0.3675i	2.4072-0.7510i
5	1	2.8162-1.1109i	2.8247-1.1084i	2.5431-0.9364i
5	2	2.5647-1.8801i	2.5724-1.8717i	2.3752-1.5833i
5	3	2.1980-2.6962i	2.1627-2.6905i	2.1144-2.2727i
5	4	1.7371-3.5727i	1.5775-3.6268i	1.7572-3.0378i
5	5	1.2034-4.5089i	0.8312-4.7548i	1.3109-3.9189i

TABLE 4.11: Low-lying ($n \leq l$, with $l = j - 3/2$ and $N = 9$) QNM frequencies using the WKB and the AIM methods for the spinor-vector perturbation potential.

l	n	3rd order WKB	6th order WKB	AIM
0	0	1.4497-0.4002i	1.4547-0.4796i	0.7104-1.6173i
1	0	1.8297-0.4125i	1.8330-0.4406i	1.5339-0.7021i
1	1	1.4203-1.3012i	1.5053-1.4296i	1.3696-1.1940i
2	0	2.1916-0.4181i	2.2015-0.4229i	1.9484-0.3686i
2	1	1.8858-1.2810i	1.9368-1.3184i	1.7584-1.1357i
2	2	1.2838-2.2713i	1.3602-2.3437i	1.3480-2.0003i
3	0	2.5450-0.4201i	2.5521-0.4198i	2.2819-0.3673i
3	1	2.3020-1.2748i	2.3396-1.2752i	2.1254-1.1156i
3	2	1.8083-2.2020i	1.8563-2.1975i	1.7843-1.9178i
3	3	1.1201-3.2730i	1.0383-3.2764i	1.2265-2.8519i
4	0	2.8944-0.4207i	2.8986-0.4198i	2.6133-0.3673i
4	1	2.6915-1.2716i	2.7162-1.2657i	2.4782-1.1102i
4	2	2.2762-2.1680i	2.3091-2.1416i	2.1886-1.8855i
4	3	1.6713-3.1673i	1.6085-3.1176i	1.7137-2.7446i
4	4	0.9407-4.2914i	0.5911-4.3139i	1.0453-3.7724i
5	0	3.2419-0.4209i	3.2443-0.4202i	2.9132-0.6496i
5	1	3.0667-1.2694i	3.0825-1.2642i	2.8247-1.1084i
5	2	2.7077-2.1489i	2.7296-2.1246i	2.5724-1.8716i
5	3	2.1727-3.1025i	2.1286-3.0438i	2.1626-2.6905i
5	4	1.5034-4.1621i	1.2338-4.1210i	1.5775-3.6268i
5	5	0.7455-5.3214i	0.0739-5.4649i	0.8312-4.7547i

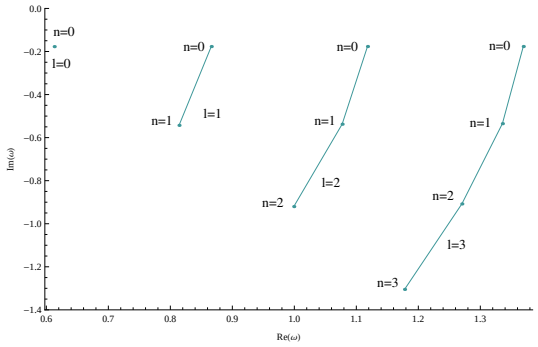

(A) QNMs associated to the 5-dimensional black hole for l=0 to l=3.

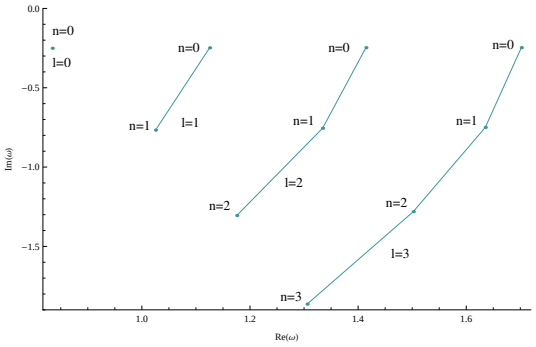

(B) QNMs associated to the 6-dimensional black hole for l=0 to l=3.

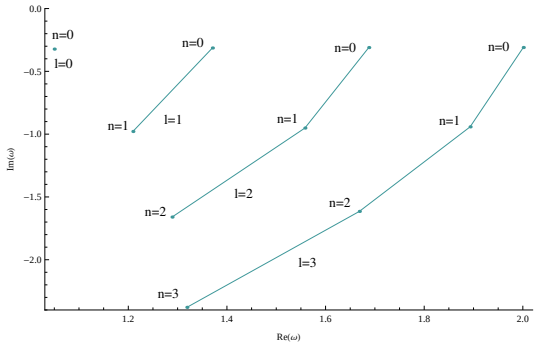

(C) QNMs associated to the 7-dimensional black hole for l=0 to l=3.

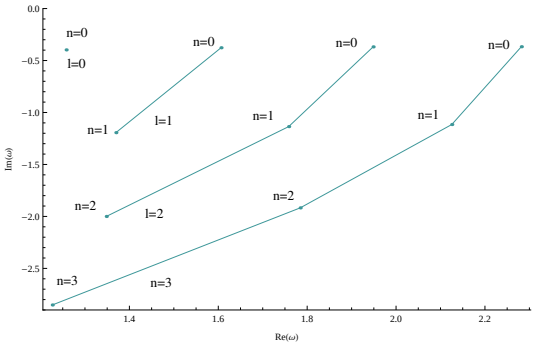

(D) QNMs associated to the 8-dimensional black hole for l=0 to l=3.

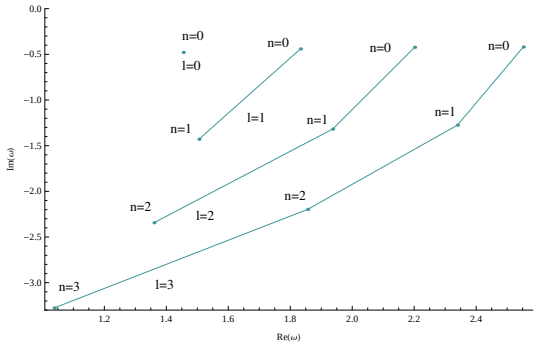

(E) QNMs associated to the 9-dimensional black hole for l=0 to l=3.

FIGURE 4.2: Low-lying ($n \leq l$, with $l = j - 3/2$ and $0 \leq l \leq 3$) gravitino QNM frequencies for spinor-vector perturbations.

The results we obtain for the spinor-vector perturbations exhibit the same trends as seen with the spinor perturbations. We see that higher dimensional black holes emit more energetic particles since the real part of the QNMs associated to them have larger values. What is interesting it that our higher dimensional black holes appear to stabilise a lot faster when compared to the lower dimensional black holes. In order to get a fuller description of collider produced black holes we need to determine the absorption probabilities associated with them. This would give us a better idea of what their

emission spectra might look like. We could also use the absorption probabilities and QNMs associated to collider produced black holes in order to determine their emission cross sections.

Chapter 5

Absorption probability

In Ch.3 we determined the potential for spinors and spinor-vectors in N-dimensional Schwarzschild space times, and in Ch.4 we obtained the allowed QNMs for these spinors and spinor-vectors. In this chapter we will determine the absorption probability associated to a field theoretic particle with energy "ω". We use two methods to do this, where we firstly introduce the Unruh method, which is used to calculate the absorption probability for particles in the low energy regime. Secondly we use the WKB method to determine the absorption probabilities for a more general energy regime. For the Unruh method we must consider the spinor and spinor-vector perturbations separately, where we will denote their respective potential functions as V and write V_1 or $\mathbb{V}_1$ where ambiguity may occur. In the case of the WKB method we can construct our absorption probability without knowing the potential and so we can consider spinor and spinor-vector perturbations simultaneously. We begin with the Unruh method for our spinor perturbation with potential function V_1 given in Eq.(3.48).

5.1 Unruh method for spinors

To implement the Unruh method we must consider three regions around the black hole: The near region, where $f(r) \to 0$, the central region, where $V(r) \gg \omega$, and the far region, where $f(r) \to 1$. Approximations are obtained for each of the regions and then coefficients are determined by comparing and evaluating the solutions at the boundaries.

Near region

In the near region $f(r) \to 0$, so Eq.(3.47) becomes

$$\left(\frac{d^2}{dr_*^2}+\omega^2\right)\widetilde{\Phi}_I=0\,, \tag{5.1}$$

which has a solution of

$$\widetilde{\Phi}_I=A_I e^{i\omega r_*}\,. \tag{5.2}$$

Central region

In this region we have that $V(r)\gg\omega$ and hence Eq.(3.47) becomes

$$\left(\frac{d}{dr_*}+W\right)\left(\frac{d}{dr_*}-W\right)\widetilde{\Phi}_{II}=0\,. \tag{5.3}$$

Defining H as

$$H=\left(\frac{d}{dr_*}-\omega\right)\widetilde{\Phi}_{II}\,, \tag{5.4}$$

the solution of Eq.(5.4) is

$$H=B_{II}\left(\frac{1+\sqrt{f}}{1-\sqrt{f}}\right)^{\frac{j}{N-3}+\frac{1}{2}}\left(\frac{\left(\frac{2}{N-2}\right)\left(j+\frac{N-3}{2}\right)-\sqrt{f}}{\left(\frac{2}{N-2}\right)\left(j+\frac{N-3}{2}\right)+\sqrt{f}}\right)\,. \tag{5.5}$$

Substituting Eq.(5.5) into Eq.(5.4), we have a first order differential equation with a solution

$$\widetilde{\Phi}_{II}=A_{II}\left(\frac{1+\sqrt{f}}{1-\sqrt{f}}\right)^{\frac{j}{N-3}+\frac{1}{2}}\left(\frac{\left(\frac{2}{N-2}\right)\left(j+\frac{N-3}{2}\right)-\sqrt{f}}{\left(\frac{2}{N-2}\right)\left(j+\frac{N-3}{2}\right)}+\sqrt{f}\right)+B_{II}\Psi\,, \tag{5.6}$$

with

$$\begin{aligned}\Psi=&\left(\frac{1+\sqrt{f}}{1-\sqrt{f}}\right)^{\frac{j}{N-3}+\frac{1}{2}}\left(\frac{\left(\frac{2}{N-2}\right)\left(j+\frac{N-3}{2}\right)-\sqrt{f}}{\left(\frac{2}{N-2}\right)\left(j+\frac{N-3}{2}\right)}+\sqrt{f}\right)\\&\times\left[\int^r\frac{1}{f}\left(\frac{1-\sqrt{f}}{1+\sqrt{f}}\right)^{\frac{2j}{N-3}+1}\left(\frac{\left(\frac{2}{N-2}\right)\left(j+\frac{N-3}{2}\right)+\sqrt{f}}{\left(\frac{2}{N-2}\right)\left(j+\frac{N-3}{2}\right)}-\sqrt{f}\right)^2 dr'\right]\,.\end{aligned} \tag{5.7}$$

Far region

In the far region $f(r)\to 1$, Eq.(3.47) becomes

$$\frac{d^2}{dr_*^2}\widetilde{\Phi}_{III}-\left[\frac{\left(\left(j+\frac{D-4}{2}\right)^2-\frac{1}{4}\right)}{r^2}-\omega^2\right]\widetilde{\Phi}_{III}=0\,. \tag{5.8}$$

In this region $r_* \sim r$, the solution can be expressed as a Bessel function

$$\widetilde{\Phi}_{III} = A_{III}\sqrt{r}J_{j+\frac{N-4}{2}}(\omega r) + B_{III}\sqrt{r}N_{j+\frac{N-4}{2}}(\omega r)\,. \tag{5.9}$$

We can set the incoming amplitude of our field $\widetilde{\Phi}_{III}$ at $r \to \infty$ to one. This gives us

$$A_{III} + iB_{III} = \sqrt{2\pi\omega}\,. \tag{5.10}$$

taking $r \to 1$ in the near region gives us that

$$A_I = A_{II}\,, \quad B_{II} = -i\omega A_I\,. \tag{5.11}$$

Comparing the solution's for regions II and III we find that the absorption probability is given as

$$|A_j(\omega)|^2 = 4\pi C^2\omega^{2j+N-3}\left(1+\pi C^2\omega^{2j+N-3}\right)^{-2} \approx 4\pi C^2\omega^{2j+N-3}\,, \tag{5.12}$$

where

$$C = \frac{1}{2^{\frac{N-1}{N-3}j+\frac{N-1}{2}}\Gamma(j+\frac{N-2}{2})}\left(\frac{j+\frac{2N-5}{2}}{j-\frac{1}{2}}\right)\,, \tag{5.13}$$

with Γ denoting the gamma function, j is our total angular momentum quantum number and ω is less than 1. Taking $N = 4$ we find that this is consistent with what we have obtained for the 4-dimensional case [31].

5.2 Unruh method for spinor-vectors

For the spinor-vector we use $\mathbb{V}_1$ given in Eq.(3.65). The method is applied in the same way as for the spinor case, so we again begin with the near region.

Near region

In this region we find that the function is the same as that for the spinor given in Eq.(5.1).

Central region

Here the wave function is

$$\widetilde{\Phi}_{II} = A_{II}\left(\frac{1+\sqrt{f}}{1-\sqrt{f}}\right)^{\frac{j}{N-3}+\frac{1}{2}} + B_{II}\Psi\,, \tag{5.14}$$

with

$$\Psi = \left(\frac{1+\sqrt{f}}{1-\sqrt{f}}\right)^{\frac{j}{N-3}+\frac{1}{2}} \left[\int^{r} \frac{1}{f}\left(\frac{1-\sqrt{f}}{1+\sqrt{f}}\right)^{\frac{2j+N-3}{N-3}} dr'\right] . \tag{5.15}$$

Far region

In this region we again find that the function is equal to that given in Eq.(5.8). This means our absorption probability is given as

$$|A(\omega)|^2 \sim \frac{4\pi\omega^{2j+N-3}}{\left(2^{\left(\left(\frac{N-1}{N-3}j+\frac{N-1}{2}\right)\right)}\Gamma\left(j+\frac{N-2}{2}\right)\right)^2} , \tag{5.16}$$

where $\omega < 1$ and j is our total angular momentum quantum number.

5.3 WKB method

Here we again rewrite Eqs.(3.47) and (3.62) as

$$\left(\frac{d^2}{dr_*^2} + Q\right)\widetilde{\Phi}_1 = 0 , \tag{5.17}$$

where $Q(r) = \omega - V(r)$ with ω representing the energy of our field and $V(r)$ representing the effective potential surrounding the black hole. For low energy particles, $\omega \ll V$, we can use the first order WKB approximation. The result for this absorption probability is given in Ref.[42]

$$|A_j| = \exp\left[-2\int_{x_1}^{x_2} \frac{dx'}{f(x')}\sqrt{-Q(x')}\right] , \tag{5.18}$$

where $x = \omega r$, and x_1 and x_2 are turning points, that is $Q(x_1) = Q(x_2) = 0$ for a given energy *omega* and potential V. For particles of energy $\omega^2 \sim V$ the formula, Eq.(5.18), no longer converges and therefore has no solution. For this energy region we will need to use a higher order WKB approximation. We use the method developed by Iyer and Will, the absorption probability is given as [23]

$$|A_j(\omega)|^2 = \frac{1}{1+e^{2S(\omega)}} , \tag{5.19}$$

where

$$\begin{aligned} S(\omega) =& \pi k^{1/2}\left[\frac{1}{2}z_0^2+\left(\frac{15}{64}b_3^2-\frac{3}{16}b_4\right)z_0^4\right] \\ &+\pi k^{1/2}\left[\frac{1155}{2048}b_3^4-\frac{315}{256}b_3^2b_4+\frac{35}{128}b_4^2+\frac{35}{64}b_3b_5-\frac{5}{32}b_6\right]z_0^6+\pi k^{-1/2}\left[\frac{3}{16}b_4-\frac{7}{64}b_3^2\right] \\ &-\pi k^{-1/2}\left[\frac{1365}{2048}b_3^4-\frac{525}{256}b_3^2b_4+\frac{85}{128}b_4^2+\frac{95}{64}b_3b_5-\frac{25}{32}b_6\right]z_0^2\,, \end{aligned} \tag{5.20}$$

and where z_0^2, b_n and k are defined by the components of the Taylor series expansion of $Q(r)$ near r_0,

$$\begin{aligned} Q &= Q_0+\frac{1}{2}Q_0''z^2+\sum_{n=3}\frac{1}{n!}\left(\frac{d^nQ}{dx^n}\right)_0 z^n \\ &= k\left[z^2-z_0^2+\sum_{n=3}b_nz^n\right], \end{aligned} \tag{5.21}$$

and

$$\begin{aligned} &z=r-r_0\,;\quad z_0^2\equiv-2\frac{Q_0}{Q_0''}\,;\quad k\equiv\frac{1}{2}Q_0''\,; \\ &b_n\equiv\left(\frac{2}{n!Q_0''}\right)\left(\frac{d^nQ}{dr_*^n}\right)_0\,;\quad \frac{d}{dr_*}=\left(1-\left(\frac{2M}{r}\right)^{N-3}\right)\frac{d}{dr}\,. \end{aligned} \tag{5.22}$$

The 0 subscripts denotes the maxima of Q and the primes denote derivatives. In Fig.5.1 we have plotted the energy ω of our particles against the absorption probability $|A(\omega)|^2$ for the 4-dimensional case for $j = 3/2, ..., 13/2$.

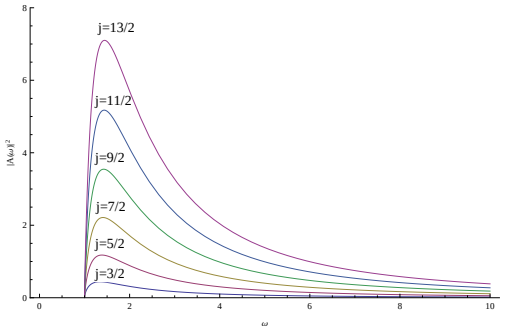

(A) Potential function for spin-3/2 particle near a 4-dimensional Schwarzschild back ground with $j = 3/2$ to $13/2$.

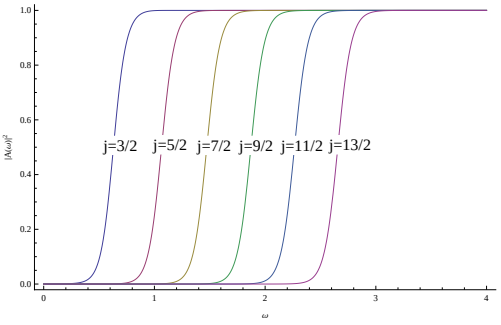

(B) Absorption probability for spin-3/2 particles for a 4-dimensional Schwarzschild black hole with $j = 3/2$ to $13/2$

FIGURE 5.1: Effective potentials and absorption probabilities for a 4-dimensional Schwarzschild black hole.

5.4 Spinor absorption probabilities

In Fig.5.1 we have set $N = 4$ and plotted the effective potential and absorption probabilites associated with the spin-3/2 particles in 4-dimensional space time. The results we obtain in both Tab.4.1 and Fig.5.1 agree with the results obtained in Ref.[31]. In Fig.5.1 $r = 2$ represents the event horizon of our black hole. It is clear from Fig.5.1 that as we increase the value of j we see that the absorption probability shifts to the right. We can also see that the Unruh method would not work for our entire energy region since when $j = 11/2$ and $13/2$ the energy required for the particle to be absorbed by the black hole is too large.

5.4.1 Higher dimensional black holes

We will now plot the effective potential and absorption probabilities for our spin-3/2 particles in space times with dimensions larger than 4.

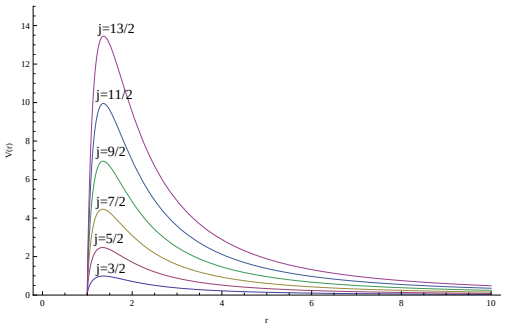

(A) Effective potential for spin-3/2 particles for a 5-dimensional Schwarzschild black hole with $j = 3/2$ to $13/2$.

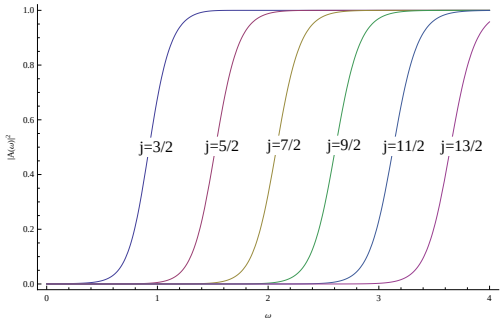

(B) Absorption probability for spin-3/2 particles for a 5-dimensional Schwarzschild black hole with $j = 3/2$ to $13/2$.

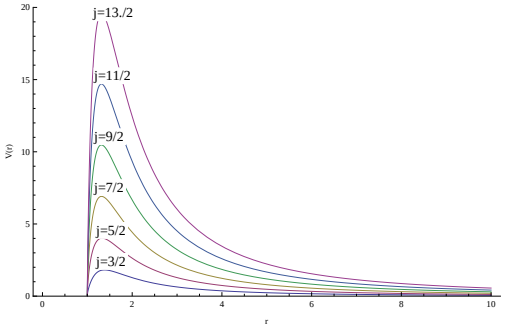

(C) Effective potential for spin-3/2 particles for a 6-dimensional Schwarzschild black hole with $j = 3/2$ to $13/2$.

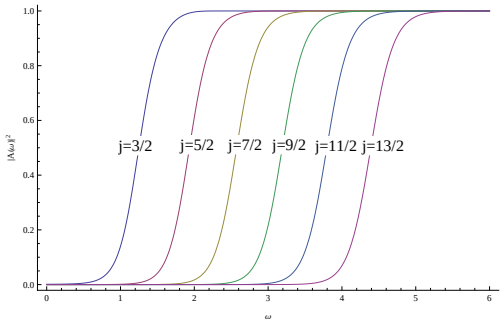

(D) Absorption probability for spin-3/2 particles for a 6-dimensional Schwarzschild black hole with $j = 3/2$ to $13/2$.

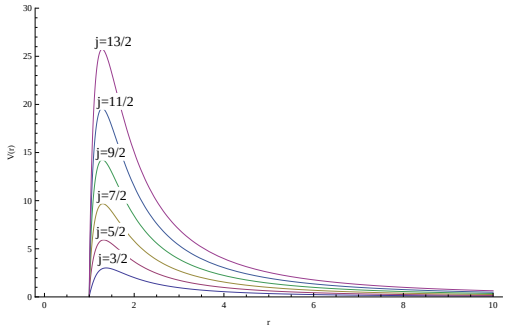

(E) Effective potential for spin-3/2 particles for a 7-dimensional Schwarzschild black hole with $j = 3/2$ to $13/2$.

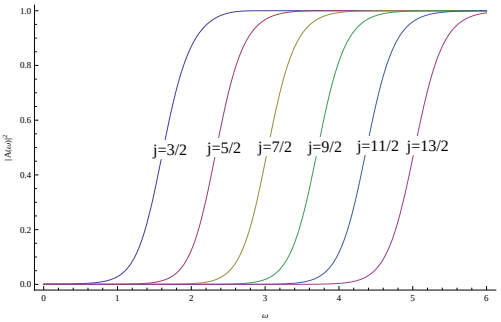

(F) Absorption probability for spin-3/2 particles for a 7-dimensional Schwarzschild black hole with $j = 3/2$ to $13/2$.

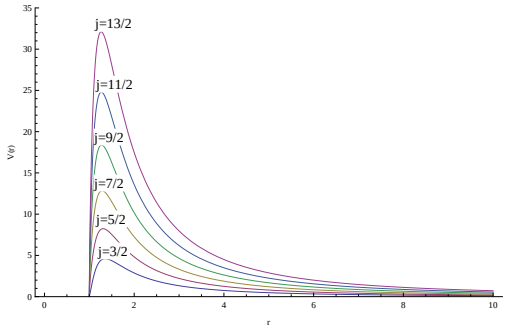

(G) Effective potential for spin-3/2 particles for a 8-dimensional Schwarzschild black hole with $j = 3/2$ to $13/2$.

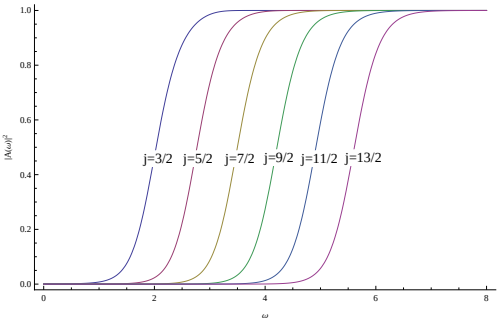

(H) Absorption probability for spin-3/2 particles for a 8-dimensional Schwarzschild black hole with $j = 3/2$ to $13/2$.

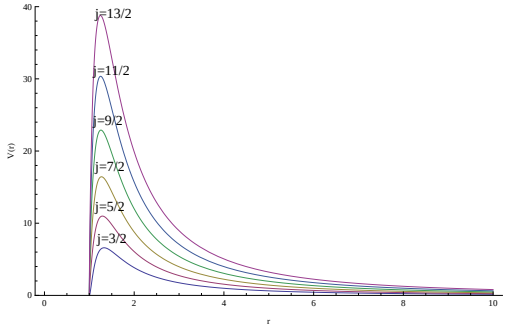

(I) Effective potential for spin-3/2 particles for a 9-dimensional Schwarzschild black hole with $j = 3/2$ to $13/2$.

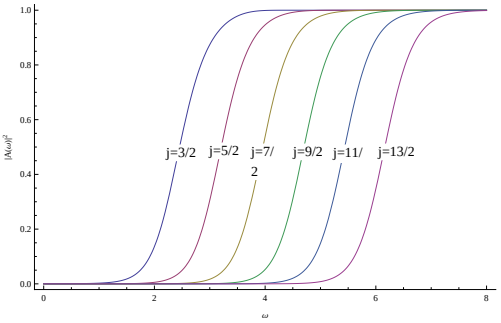

(J) Absorption probability for spin-3/2 particles for a 9-dimensional Schwarzschild black hole with $j = 3/2$ to $13/2$.

FIGURE 5.2: Effective potentials and absorption probabilities for higher dimensional Schwarzschild black holes.

Fig.5.2 clearly shows that particles with larger j quantum numbers require more energy to be absorbed by black holes. We do see, however, that all particles of the same dimension change from total reflection to total absorption in a very similar way, regardless of their j quantum number. These results agree with those obtained in Ref.[43]

5.4.2 Comparisons between j

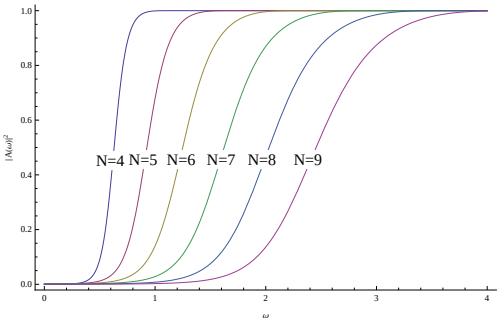

(A) Absorption probabilities for spin-3/2 particles near Schwarzschild black holes with $j = 3/2$ in various dimensions.

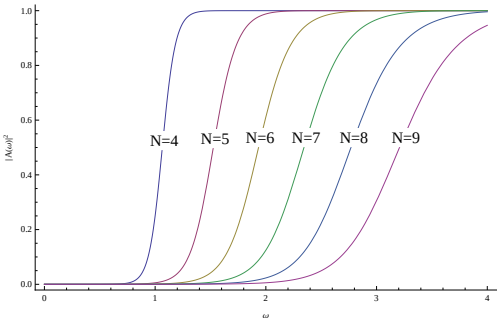

(B) Absorption probabilities for spin-3/2 particles near Schwarzschild black holes with $j = 5/2$ in various dimensions.

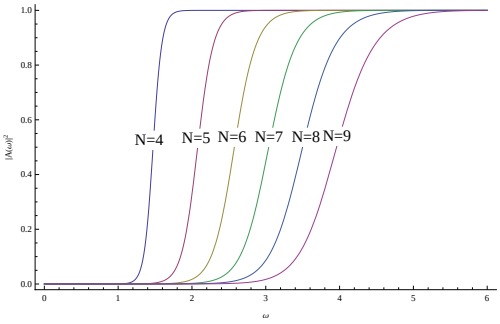

(C) Absorption probabilities for spin-3/2 particles near Schwarzschild black holes with $j = 7/2$ in various dimensions.

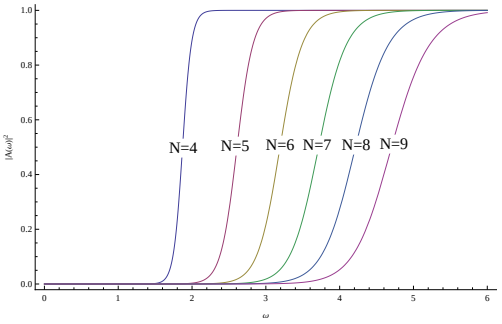

(D) Absorption probabilities for spin-3/2 particles near Schwarzschild black holes with $j = 9/2$ in various dimensions.

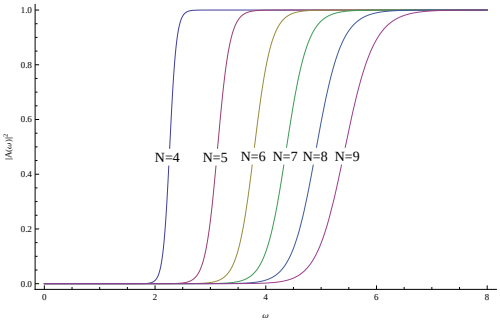

(E) Absorption probabilities for spin-3/2 particles near Schwarzschild black holes with $j = 11/2$ in various dimensions.

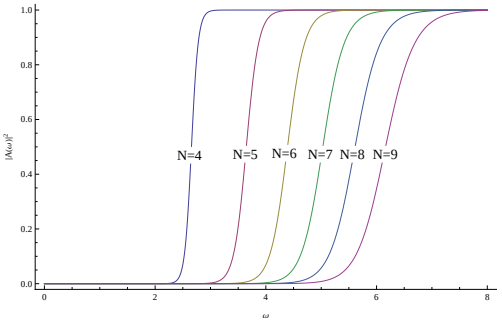

(F) Absorption probabilities for spin-3/2 particles near Schwarzschild black holes with $j = 13/2$ in various dimensions.

FIGURE 5.3: Absorption probabilities associated to spin-3/2 particles with various values of j.

We again see that an increase in dimensions results in an increase in energy of emitted particles. More interestingly though, we can see that higher dimensional black holes have a tendency to have a larger energy range from total reflection to total absorption.

5.5 Spinor-vector absorption probabilities

We apply the same procedure as we have done for the spinor potential, although this time we use $\mathbb{V}_1$. Here we cannot determine the absorption probability for the 4-dimensional case, since as discussed in Ch.2 we do not have any "TT eigenmodes" for space time dimensions lower than 5. Plotting these results we see the same patterns as we have seen for the spinors in our N-dimensional space. It should be noted that we do see that the spinor-vectors tend to have a lower energy emission when compared to the spinors.

5.5.1 Higher dimensional black holes

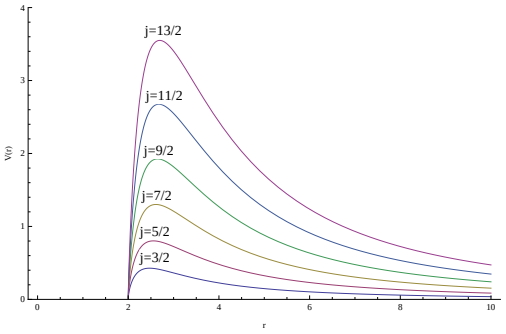

(A) Effective potential for spin-3/2 particles for a 5-dimensional Schwarzschild black hole with $j = 3/2$ to $13/2$.

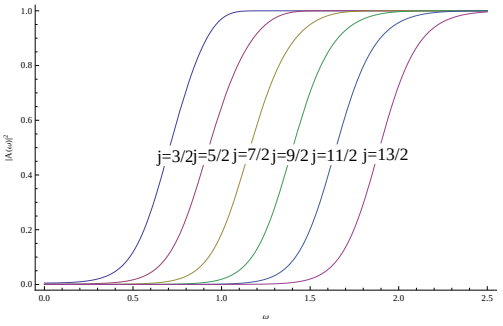

(B) Absorption probability for spin-3/2 particles for a 5-dimensional Schwarzschild black hole with $j = 3/2$ to $13/2$.

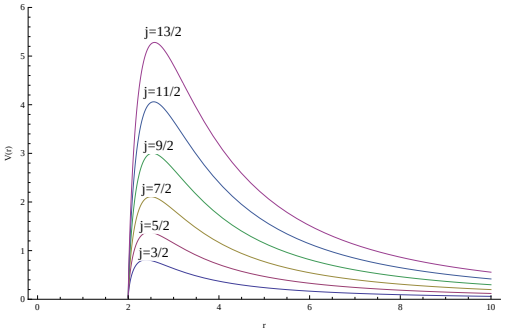

(C) Effective potential for spin-3/2 particles for a 6-dimensional Schwarzschild black hole with $j = 3/2$ to $13/2$.

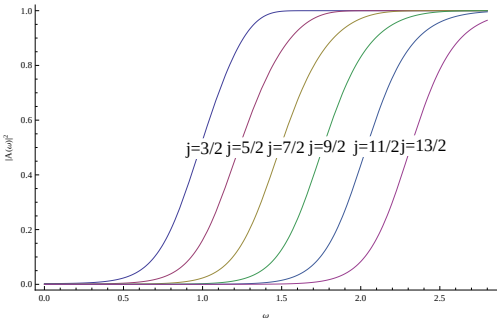

(D) Absorption probability for spin-3/2 particles for a 6-dimensional Schwarzschild black hole with $j = 3/2$ to $13/2$.

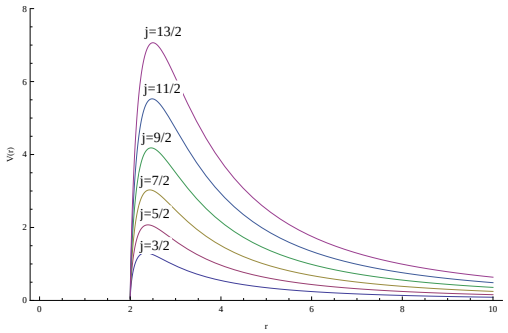

(E) Effective potential for spin-3/2 particles for a 7-dimensional Schwarzschild black hole with $j = 3/2$ to $13/2$.

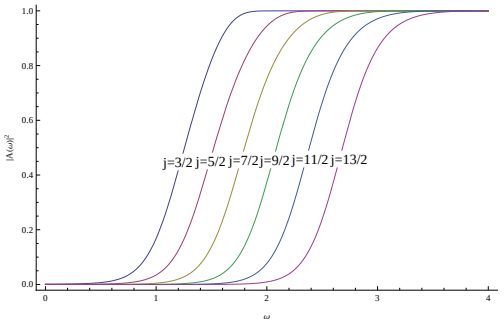

(F) Absorption probability for spin-3/2 particles for a 7-dimensional Schwarzschild black hole with $j = 3/2$ to $13/2$.

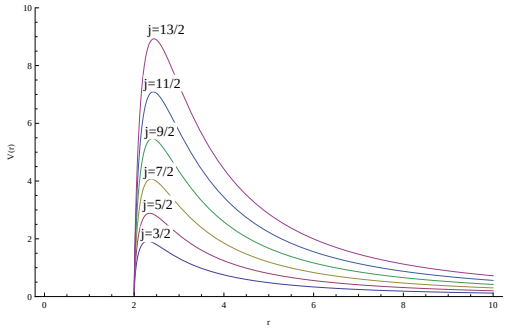

(G) Effective potential for spin-3/2 particles for a 8-dimensional Schwarzschild black hole with $j = 3/2$ to $13/2$.

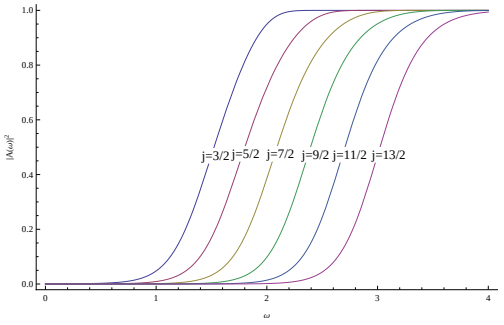

(H) Absorption probability for spin-3/2 particles for a 8-dimensional Schwarzschild black hole with $j = 3/2$ to $13/2$.

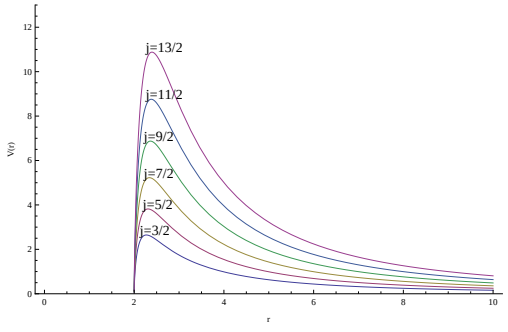

(I) Effective potential for spin-3/2 particles for a 9-dimensional Schwarzschild black hole with $j = 3/2$ to $13/2$.

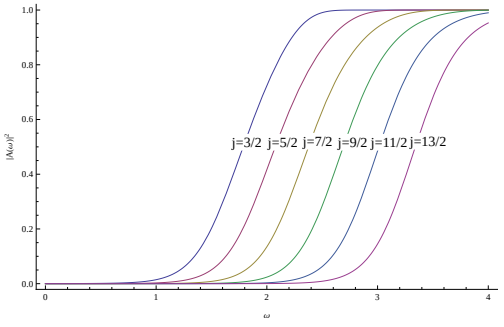

(J) Absorption probability for spin-3/2 particles for a 9-dimensional Schwarzschild black hole with $j = 3/2$ to $13/2$.

FIGURE 5.4: Effective potential and absorption probabilities for Spinor-vectors in higher dimensional space times near Schwarzschild black holes.

5.5.2 Comparisons between j

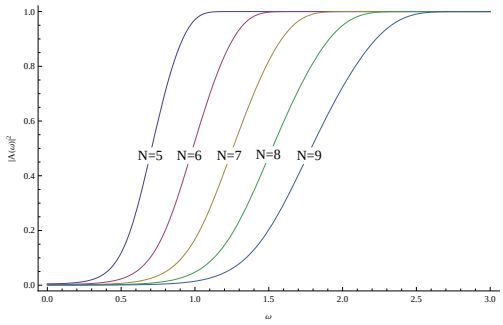

(A) Absorption probability for spin-3/2 particles for $j = 3/2$ in various dimensional Schwarzschild black hole space times

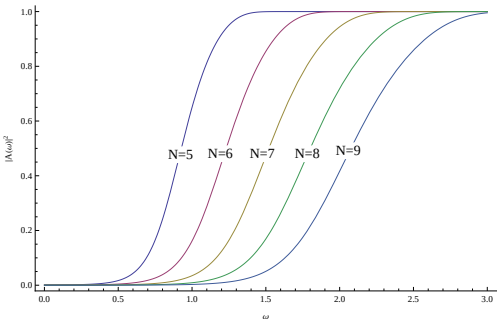

(B) Absorption probability for spin-3/2 particles for $j = 5/2$ in various dimensional Schwarzschild black hole space times

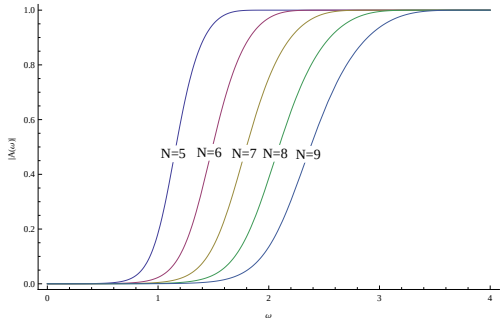

(C) Absorption probability for spin-3/2 particles for $j = 7/2$ in various dimensional Schwarzschild black hole space times

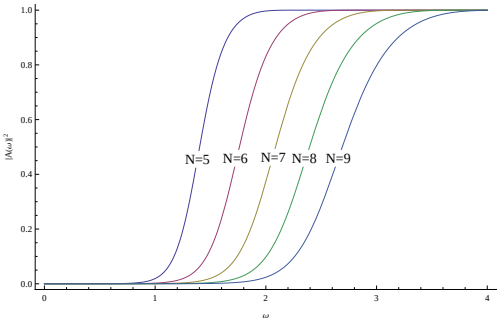

(D) Absorption probability for spin-3/2 particles for $j = 9/2$ in various dimensional Schwarzschild black hole space times

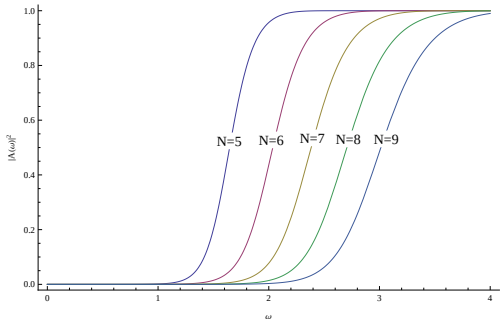

(E) Absorption probability for spin-3/2 particles for $j = 11/2$ in various dimensional Schwarzschild black hole space times

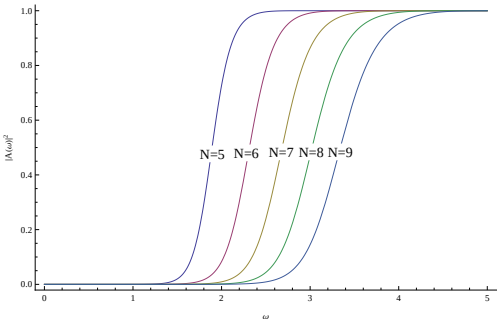

(F) Absorption probability for spin-3/2 particles for $j = 13/2$ in various dimensional Schwarzschild black hole space times

FIGURE 5.5: Absorption probabilities for Spinor-vectors of spin-3/2 particles with various values of j

We see the same trends in Figs.5.4 and 5.5 as we saw for the spinor results. We also note that our energies for the spinor-vectors are much smaller than those of the spinors.

The results that we obtain in Figs.5.4 and 5.5 are exactly the same as those obtained for the spin-1/2 particles near N-dimensional Schwarzschild black holes [32].

Chapter 6

Concluding remarks

In this dissertation we have shown that it is possible to exploit the radial symmetry surrounding a Schwarzschild black hole in order to determine the effective potential felt by spin-3/2 particles near the black hole. In order to do this we firstly needed to determine the eigenvalues and eigenfunctions for our spinor-vectors on S^N. We present the complete set of eigenvalues and eigenfunctions in Ch.2. The eigenvalues for our non TT eigenspinor-vectors are given in Eq.(2.27) and the respective eigenfunctions in Eq.(2.28). The eigenvalues for our TT eigenspinor-vectors are given in Eq.(2.55).

In Ch.3 we determine the effective potentials for our non TT eigenspinor-vectors, Eq.(3.48), and our TT eigenspinor-vectors, Eq.(3.65). Setting the number of dimensions to 4 for non TT eigenmodes gives us the potential that we have derived in Ref.[31]. We also note that the potentials obtained for our TT eigenmodes are identical to those of the Dirac fermionic case as seen in Ref.[32].

We have then used the effective potentials developed in Ch.3 to determine the numerical values of the QNMs for our emitted spin-3/2 particles. We use the WKB method, to 3rd and 6th order, and the Improved AIM to determine these results and present them in Ch.4. We note that there is a general trend in our QNMs as we increase the number of dimensions. That is, the real parts of our QNMs increase for particles emitted by higher dimensional black holes. We also note that there exists a tendency for particles with larger j quantum numbers to have associated with them larger imaginary parts for their QNMs.

Finally, in Ch.5 we present the Unruh method in order to calculate the absorption probabilities of our black holes for our low energy particles. We then describe how the WKB method can be used to determine the absorption probabilities for a more general energy regime. We then present the absorption probabilities associated to our spin-3/2 fields for both the spinor and spinor-vector perturbations.

The results we obtain for the QNMs and the absorption probabilities would be useful in

trying to detect and understand the production and evolution of collider produced black holes [2], where detection of QNMs would prove the existence of higher dimensional black holes and allow us to determine the mass of the black hole that emitted them.

6.1 Future works

We hope to extend the work that we have done on the Schwarzschild black hole to the case of other spherically symmetrical black hole space times. An interesting topic of research would be to investigate the (A)ds-Schwarzschild space time, since as discussed in Ch.3 this would be a non-flat Ricci space time.
Another interesting space time would be the Reissner-Nordström black hole, since here we would have to include the electromagnetic tensor to our covariant derivative (we present the calculation of this in App.A). Furthermore, it has been shown that for the extremal 4-dimensional Reissner-Nordtröm black hole the QNM frequencies are the same for spin-0, 1/2, 3/2 and 2 [44]. We would like to see if this is true for higher dimensional extremal Reissner-Nordström black holes.

Appendix A

Dirac operators in other space times

In Ch.3 we looked for a gauge invariant form of our eigenspinors and required that for systems with only gravitational forces

$$\gamma^{\mu\nu\alpha}\nabla_\nu\nabla_\alpha\varphi = \frac{1}{8}\gamma^{\mu\nu\alpha}R_{\nu\alpha\rho\sigma}\gamma^\rho\gamma^\alpha\varphi\,, \tag{A.1}$$

in order for our spinors to transform as

$$\psi'_\mu = \psi_\mu + \nabla_\mu\varphi\,. \tag{A.2}$$

Here we will present a method and solution for finding our covariant derivative when we consider both gravitational forces and electric charge, in this case we must include the electromagnetic field tensor. We make the *ansatz* that our covariant derivative is given as

$$\nabla_\mu = \widetilde{\nabla}_\mu + a\sqrt{\Lambda}\gamma_\mu + b\gamma^\rho F_{\mu\rho} + c\gamma_{\mu\rho\sigma}F^{\rho\sigma}\,, \tag{A.3}$$

where a, b, c and Λ are constants to be determined, and $\widetilde{\nabla}_\mu$ is the covariant derivative in the uncharged space time. We consider again the transformation of our spinor as

$$\psi'_\mu = \psi_\mu + \nabla_\mu\varphi\,. \tag{A.4}$$

Plugging this into the Rarita-Schwinger equation gives

$$\begin{aligned}\gamma^{\lambda\mu\nu}\nabla_\mu\psi'_\nu &= 0\\ \gamma^{\lambda\mu\nu}\nabla_\mu\left(\psi_\nu + \nabla_\nu\varphi\right) &= 0\,.\end{aligned} \tag{A.5}$$

This implies that

$$\gamma^{\lambda\mu\nu}\nabla_\mu\nabla_\nu\varphi = 0\,, \tag{A.6}$$

but now

$$\gamma^{\lambda\mu\nu}\nabla_\mu\nabla_\nu\varphi = \frac{1}{2}\gamma^{\lambda\mu\nu}\left[\nabla_\mu,\nabla_\nu\right]\varphi\,. \tag{A.7}$$

So in order to determine our unknown constants we must solve the equation of

$$\gamma^{\lambda\mu\nu}\left[\nabla_\mu,\nabla_\nu\right]\varphi = 0\,. \tag{A.8}$$

The details of this calculation are lengthy and we will not present the solution in its entirety, as we are required to determine summations over gamma matrices and covariant derivatives for 16 separate terms. Solving this, however, gives us that the covariant derivative is written as [45]

$$\nabla_\mu = \widetilde{\nabla}_\mu + \frac{m}{2}\gamma_\mu - 2ia\left(N-2\right)\partial^\mu_\mu\gamma^\rho F_{\mu\rho} + ia\gamma_{\mu\rho\sigma}F^{\rho\sigma}\,, \tag{A.9}$$

where

$$a = \frac{1}{4\sqrt{2(N-1)(N-2)}} \quad \text{and} \quad m = \frac{4}{\sqrt{2(N-1)(N-2)}}e \tag{A.10}$$

with e a gauge coupling constant.

Bibliography

[1] CMS *et al.*, CMS PAS EXO-15-004 (Dec. 2015) (2015).

[2] P. Kanti, in *Physics of Black Holes* (Springer, 2009) pp. 387–423.

[3] A. M. Steane, arXiv:math-ph/1312.3824 .

[4] A. Bilal, arXiv:hep-th/0101055 (2001).

[5] D. Griffiths, *Introduction to elementary particles* (John Wiley & Sons, 2008).

[6] I. Aitchison, *Supersymmetry in particle physics: an elementary introduction* (Cambridge University Press, 2007).

[7] H. Nastase, arXiv:hep-th/1112.3502 (2011).

[8] L. Parker, in *Journal of Physics: Conference Series*, Vol. 600 (IOP Publishing, 2015) p. 012001.

[9] T. Moroi, H. Murayama, and M. Yamaguchi, Physics Letters B **303**, 289 (1993).

[10] R. Barbieri and G. F. Giudice, Nuclear Physics B **306**, 63 (1988).

[11] F. Takayama and M. Yamaguchi, Physics Letters B **485**, 388 (2000).

[12] T. Banks and W. Fischler, arXiv:hep-th/9906038 (1999).

[13] S. B. Giddings and S. Thomas, Physical Review D **65**, 056010 (2002).

[14] S. Dimopoulos and G. Landsberg, Physical Review Letters **87**, 161602 (2001).

[15] A. F. Ali, M. Faizal, and M. M. Khalil, Physics Letters B **743**, 295 (2015).

[16] S. Funkhouser, in *Proceedings of the Royal Society of London A: Mathematical, Physical and Engineering Sciences*, Vol. 466 (The Royal Society, 2010) pp. 1155–1166.

[17] W. Unruh, Physical Review D **14**, 3251 (1976).

[18] T. Regge and J. A. Wheeler, Physical Review **108**, 1063 (1957).

[19] C. V. Vishveshwara, Nature **227**, 936 (1970).

[20] K. D. Kokkotas and B. G. Schmidt, Living Rev. Rel **2**, 262 (1999).

[21] G. E. Harmsen, in *Journal of Physics: Conference Series*, Vol. 645 (IOP Publishing, 2015) p. 012003.

[22] D. J. Griffiths and E. G. Harris, *Introduction to quantum mechanics*, Vol. 2 (Prentice Hall New Jersey, 1995).

[23] S. Iyer and C. M. Will, Physical Review D **35**, 3621 (1987).

[24] R. Konoplya, Physical Review D **68**, 024018 (2003).

[25] H. Ciftci, R. L. Hall, and N. Saad, Journal of Physics A: Mathematical and General **36**, 11807 (2003).

[26] H.-T. Cho, A. S. Cornell, J. Doukas, T. R. Huang, and W. Naylor, Advances in Mathematical Physics **2012**, 281705 (2012).

[27] R. Camporesi and A. Higuchi, Journal of Geometry and Physics **20**, 1 (1996).

[28] L. Parker and D. Toms, *Quantum field theory in curved spacetime: quantized fields and gravity* (Cambridge University Press, 2009).

[29] C.-H. Chen, H.-T. Cho, A. S. Cornell, and G. E. Harmsen, (2016), arXiv:1605.05263 [gr-qc] .

[30] W. Rarita and J. Schwinger, Physical Review **60**, 61 (1941).

[31] C.-H. Chen, H.-T. Cho, A. S. Cornell, G. E. Harmsen, and W. Naylor, Chinese Journal Of Physics **53** (2015).

[32] H. Cho, A. Cornell, J. Doukas, and W. Naylor, Physical Review D **75**, 104005 (2007).

[33] H. Kodama and A. Ishibashi, Progress of theoretical physics **110**, 701 (2003).

[34] H. Kodama and M. Sasaki, Progress of Theoretical Physics Supplement **78**, 1 (1984).

[35] B. Abbott, R. Abbott, T. Abbott, M. Abernathy, F. Acernese, K. Ackley, C. Adams, T. Adams, P. Addesso, R. Adhikari, *et al.*, Physical Review Letters **116**, 061102 (2016).

[36] C. M. Harris, M. J. Palmer, M. A. Parker, P. Richardson, A. Sabetfakhri, and B. R. Webber, Journal of High Energy Physics **2005**, 053 (2005).

[37] H.-T. Cho, A. Cornell, J. Doukas, and W. Naylor, Physical Review D **80**, 064022 (2009).

[38] J. Doukas, H. Cho, A. Cornell, and W. Naylor, Physical Review D **80**, 045021 (2009).

[39] H.-T. Cho, A. Cornell, J. Doukas, and W. Naylor, Classical and Quantum Gravity **27**, 155004 (2010).

[40] G. Gibbons and S. A. Hartnoll, Phys. Rev. **D66**, 064024 (2002).

[41] O. P. Fernandez Piedra, International Journal of Modern Physics D **20**, 93 (2011).

[42] H.-T. Cho and Y. Lin, Classical and Quantum Gravity **22**, 775 (2005).

[43] G. E. Harmsen, C.-H. Chen, H.-T. Cho, and A. S. Cornell, Workshop on High Energy Particle Physics (HEPPW2016) Johannesburg (2016).

[44] H.-T. Cho, Physical Review D **73**, 024019 (2006).

[45] J. T. Liu, L. A. P. Zayas, and Z. Yang, Journal of High Energy Physics **2014**, 1 (2014).